group in both low-GCS and control mice (Figure 5A). Pretreatment with SM-31900 significantly reduced infarct volume in C57BL/6 and low-GCS mice by 35% and 42%, respectively (control C57BL/6, 46.3 ±18.6 mm^3; low-GCS mice, 69.8±24.4 mm^3; Figure 5B). Physiological parameters during ischemic experiment are summarized in supplemental Table I, available online at http://stroke.ahajournals.org.

Discussion

We generated 2 transgenic mouse lines with genetically altered GCS activities, ie, high-GCS and low-GCS mice, and examined neural injury after MCA occlusion by monitoring concentrations of extracellular amino acids. Low-GCS mice had higher extracellular glycine concentrations and larger infarct volumes than did control mice. In sharp contrast, high-GCS mice had lower extracellular glycine levels and smaller infarct volumes. In the development of ischemic injury, a high extracellular concentration of glutamate is known to be neurotoxic,[2,21] whereas GABA plays a neuroprotective role.[22] In our experiments, no significant differences in extracellular glutamate or GABA concentrations were observed among the 3 mouse groups with distinct extracellular glycine concentrations. These results demonstrated a direct correlation between neuronal injury and extracellular glycine concentration, which is maintained by the GCS.

Glycine plays 2 important roles in the central nervous system: that of an inhibitory neurotransmitter and that of a modulator of excitation at the NMDA receptor. The infarct volume in low-GCS mice was markedly reduced by administration of an antagonist of the NMDA receptor glycine site. One possible explanation for this result is that low GCS activity affected ischemic damage mainly via the NMDA receptor. Lower GCS activity caused a higher extracellular glycine concentration, which resulted in overexcitation of NMDA receptors, leading to more severe ischemic injury. If SM-31900 had completely blocked the glycine site of the NMDA receptor, then infarct volume in SM-31900–treated wild-type mice would have been similar to that of SM-31900–treated, low-GCS mice. However, infarct volume in SM-31900–treated, low-GCS mice was similar to that of untreated, wild-type mice (Figure 5), which may suggest partial blocking of the glycine site by SM-31900 or the presence of another neuroprotective effect of SM-31900 that remains unidentified. At this moment, we cannot exclude the possibility that the altered GCS activity affected neural injury via inhibitory glycine receptors. Further study is required to understand the mechanism underlying a direct correlation between ischemic injury and extracellular glycine concentrations.

It is an old but still open question whether the glycine site of the NMDA receptor is saturated under physiological conditions.[23,24] Glycine is normally present in brain interstitial space at a concentration of 4 μmol/L in the cortex and 1 μmol/L in the striatum.[6,25] The NMDA-associated glycine-binding site is fully saturated at a glycine concentration of <1 μmol/L, suggesting that the glycine site of the NMDA receptor should be saturated under physiological conditions.[5] In line with these results, high extracellular glycine concentrations failed to potentiate NMDA-evoked depolarization in vivo by microdialysis with extracellular field potential recording.[7] Many in vivo studies have nevertheless demonstrated protective effects of NMDA glycine site antagonists.[9,24] In this study, we showed that infarct volume was larger in mice with higher extracellular glycine concentrations and that neural injury was ameliorated by an NMDA glycine site antagonist. Recently, we found that low-GCS mice had behavioral abnormalities such as hyperactivity and increased aggression. These phenotypes resemble the symptoms of patients with a mild form GE, who do not manifest neonatal seizures or coma but instead have behavioral abnormalities.[26] Thus far, these observations support the notion that the glycine-binding site of the NMDA receptor is not functionally saturated under physiological conditions and that the NMDA receptor could respond to changes in extracellular glycine concentrations.

Extracellular glycine reached its highest peak during MCA occlusion in low-GCS mice compared with controls (Figure 3A). Ischemia-induced acidosis leads to dysfunction of the glycine transporter, which triggers an efflux of intracellular glycine into the extracellular space.[27] The higher peak was probably due to a higher intracellular glycine content in the striatum in low-GCS mice (Figure 2B). The peak glycine level in high-GCS mice was not lower than that in controls 50 to 60 minutes after MCA occlusion, which may be explained by the fact that the glycine content in the striatum did not significantly differ between high-GCS and wild-type mice (Figure 2B). The elevated glycine level was normalized more rapidly in high-GCS mice compared with low-GCS and wild-type mice (Figure 3). Total glycine release during the first 2 hours after ischemia may affect the extent of ischemic injury rather than the glycine concentration at each time point.

An antagonist of the glycine site of the NMDA receptor, SM-31900, ameliorated ischemic injury in high-GCS mice, in accordance with a previous report that SM-31900 attenuated neuronal injury in a rat model of focal ischemia.[19] A number of antagonists for the glycine site of the NMDA receptor have been developed to date.[9] Clinical trials with some of the antagonists have been performed, but so far, these have proven unsuccessful. The infarct size in high-GCS mice (56.5±7.94 mm^3) was comparable to that of SM-31900–treated, wild-type C57BL/6 mice (46.3±18.6 mm^3) as shown in Figures 4C and 5B, suggesting that the enhancement of GCS activity has a similar neuroprotective effect. If a small molecule that enhances GCS activity were to become available, it could be used as a neuroprotective drug for various NMDA receptor–related neurodegenerative disorders. The low-GCS and high-GCS mouse lines established in the current study would be valuable tools for studying the effect of extracellular glycine concentrations in vivo.

Sources of Funding

This work was supported by a grant from the Ministry of Education, Culture, Sports, Science, and Technology in Japan (No.17591067 to S.K. and No.17591497 to H.K.).

Disclosures

None.

References

1. Graham SH, Shiraishi K, Panter SS, Simon RP, Faden AI. Changes in extracellular amino acid neurotransmitters produced by focal cerebral ischemia. *Neurosci Lett.* 1990;110:124–130.

2. Lipton SA, Rosenberg PA. Excitatory amino acids as a final common pathway for neurologic disorders. *N Engl J Med.* 1994;330:613–622.
3. Betz H, Langosch D, Hoch W, Prior P, Pribilla I, Kuhse J, Schmieden V, Malosio ML, Matzenbach B, Holzinger F, et al. Structure and expression of inhibitory glycine receptors. *Adv Exp Med Biol.* 1991;287:421–429.
4. Johnson JW, Ascher P. Glycine potentiates the NMDA response in cultured mouse brain neurons. *Nature.* 1987;325:529–531.
5. Newell DW, Barth A, Ricciardi TN, Malouf AT. Glycine causes increased excitability and neurotoxicity by activation of NMDA receptors in the hippocampus. *Exp Neurol.* 1997;145:235–244.
6. Shimizu-Sasamata M, Bosque-Hamilton P, Huang PL, Moskowitz MA, Lo EH. Attenuated neurotransmitter release and spreading depression-like depolarizations after focal ischemia in mutant mice with disrupted type I nitric oxide synthase gene. *J Neurosci.* 1998;18:9564–9571.
7. Obrenovitch TP, Hardy AM, Urenjak J. High extracellular glycine does not potentiate *N*-methyl-D-aspartate-evoked depolarization in vivo. *Brain Res.* 1997;746:190–194.
8. Zhao P, Qian H, Xia Y. GABA and glycine are protective to mature but toxic to immature rat cortical neurons under hypoxia. *Eur J Neurosci.* 2005;22:289–300.
9. Jansen M, Dannhardt G. Antagonists and agonists at the glycine site of the NMDA receptor for therapeutic interventions. *Eur J Med Chem.* 2003;38:661–670.
10. Patel J, Zinkand WC, Thompson C, Keith R, Salama A. Role of glycine in the NMDA-mediated neuronal cytotoxicity. *J Neurochem.* 1990;54: 849–854.
11. Zafra F, Aragon C, Gimenez C. Molecular biology of glycinergic neurotransmission. *Mol Neurobiol.* 1997;14:117–142.
12. Sato K, Yoshida S, Fujiwara K, Tada K, Tohyama M. Glycine cleavage system in astrocytes. *Brain Res.* 1991;567:64–70.
13. Sakata Y, Owada Y, Sato K, Kojima K, Hisanaga K, Shinka T, Suzuki Y, Aoki Y, Satoh J, Kondo H, Matsubara Y, Kure S. Structure and expression of the glycine cleavage system in rat central nervous system. *Brain Res Mol Brain Res.* 2001;94:119–130.
14. Kikuchi G. The glycine cleavage system: composition, reaction mechanism, and physiological significance. *Mol Cell Biochem.* 1973;1: 169–187.
15. Kure S, Kato K, Dinopoulos A, Gail C, Degrauw TJ, Christodoulou J, Bzduch V, Kalmanchey R, Fekete G, Trojovsky A, Plecko B, Breningstall G, Tohyama J, Aoki Y, Matsubara Y. Comprehensive mutation analysis of GLDC, AMT, and GCSH in nonketotic hyperglycinemia. *Hum Mutat.* 2006;27:343–352.
16. Kure S, Narisawa K, Tada K. Structural and expression analyses of normal and mutant mRNA encoding glycine decarboxylase: three-base deletion in mRNA causes nonketotic hyperglycinemia. *Biochem Biophys Res Commun.* 1991;174:1176–1182.
17. Niwa H, Yamamura K, Miyazaki J. Efficient selection for high-expression transfectants with a novel eukaryotic vector. *Gene.* 1991;108: 193–199.
18. Kamii H, Kinouchi H, Sharp FR, Koistinaho J, Epstein CJ, Chan PH. Prolonged expression of hsp70 mRNA following transient focal cerebral ischemia in transgenic mice overexpressing CuZn-superoxide dismutase. *J Cereb Blood Flow Metab.* 1994;14:478–486.
19. Ohtani K, Tanaka H, Ohno Y. SM-31900, a novel NMDA receptor glycine-binding site antagonist, reduces infarct volume induced by permanent middle cerebral artery occlusion in spontaneously hypertensive rats. *Neurochem Int.* 2003;42:375–384.
20. Kinouchi H, Epstein CJ, Mizui T, Carlson E, Chen SF, Chan PH. Attenuation of focal cerebral ischemic injury in transgenic mice overexpressing CuZn superoxide dismutase. *Proc Natl Acad Sci U S A.* 1991;88: 11158–11162.
21. Choi DW, Rothman SM. The role of glutamate neurotoxicity in hypoxic-ischemic neuronal death. *Annu Rev Neurosci.* 1990;13:171–182.
22. Madden KP. Effect of γ-aminobutyric acid modulation on neuronal ischemia in rabbits. *Stroke.* 1994;25:2271–2274; discussion 2274–2275.
23. Wood PL. The co-agonist concept: is the NMDA-associated glycine receptor saturated in vivo? *Life Sci.* 1995;57:301–310.
24. Danysz W, Parsons AC. Glycine and *N*-methyl-D-aspartate receptors: physiological significance and possible therapeutic applications. *Pharmacol Rev.* 1998;50:597–664.
25. Globus MY, Busto R, Martinez E, Valdes I, Dietrich WD, Ginsberg MD. Comparative effect of transient global ischemia on extracellular levels of glutamate, glycine, and γ-aminobutyric acid in vulnerable and nonvulnerable brain regions in the rat. *J Neurochem.* 1991;57:470–478.
26. Dinopoulos A, Kure S, Chuck G, Sato K, Gilbert DL, Matsubara Y, Degrauw T. Glycine decarboxylase mutations: a distinctive phenotype of nonketotic hyperglycinemia in adults. *Neurology.* 2005;64:1255–1257.
27. Swanson RA, Ying W, Kauppinen TM. Astrocyte influences on ischemic neuronal death. *Curr Mol Med.* 2004;4:193–205.

Available online at www.sciencedirect.com
ScienceDirect
Molecular Genetics and Metabolism 91 (2007) 384–389
Molecular Genetics and Metabolism
www.elsevier.com/locate/ymgme

Allelic and non-allelic heterogeneities in pyridoxine dependent seizures revealed by *ALDH7A1* mutational analysis

Junko Kanno [a], Shigeo Kure [a,*], Ayumi Narisawa [a], Fumiaki Kamada [a], Masaru Takayanagi [b], Katsuya Yamamoto [b], Hisao Hoshino [c], Tomohide Goto [d], Takao Takahashi [e], Kazuhiro Haginoya [f], Shigeru Tsuchiya [f], Fritz A.M. Baumeister [g], Yuki Hasegawa [h], Yoko Aoki [a], Seiji Yamaguchi [h], Yoichi Matsubara [a]

[a] *Department of Medical Genetics, Tohoku University School of Medicine, 1-1 Seiryomachi, Aobaku, Sendai 980-8574, Japan*
[b] *Department of Pediatrics, Sendai City Hospital, Sendai, Japan*
[c] *Department of Pediatrics, Hitachi General Hospital, Hitachi, Japan*
[d] *Department of Neurology, Tokyo Metropolitan Kiyose Children's Hospital, Tokyo, Japan*
[e] *Department of Pediatrics, Keio University School of Medicine, Tokyo, Japan*
[f] *Department of Pediatrics, Tohoku University School of Medicine, Sendai, Japan*
[g] *Neuropediatrics, Children's Hospital of the Technical University Munich, Munich, Germany*
[h] *Department of Pediatrics, Shimane University, Faculty of Medicine, Izumo, Japan*

Received 15 February 2007; accepted 15 February 2007
Available online 11 April 2007

Abstract

Pyridoxine dependent seizure (PDS) is a disorder of neonates or infants with autosomal recessive inheritance characterized by seizures, which responds to pharmacological dose of pyridoxine. Recently, mutations have been identified in the ALDH7A1 gene in Caucasian families with PDS. To elucidate further the genetic background of PDS, we screened for *ALDH7A1* mutations in five PDS families (patients 1–5) that included four Orientals. Diagnosis as having PDS was confirmed by pyridoxine-withdrawal test. Exon sequencing analysis of patients 1–4 revealed eight *ALDH7A1* mutations in compound heterozygous forms: five missense mutations, one nonsense mutation, one point mutation at the splicing donor site in intron 1, and a 1937-bp genomic deletion. The deletion included the entire exon 17, which was flanked by two *Alu* elements in introns 16 and 17. None of the mutations was found in 100 control chromosomes. In patient 5, no mutation was found by the exon sequencing analysis. Furthermore, expression level or nucleotide sequences of *ALDH7A1* mRNA in lymphoblasts were normal. Plasma pipecolic acid concentration was not elevated in patient 5. These observations suggest that *ALDH7A1* mutation is unlikely to be responsible for patient 5. Abnormal metabolism of GABA/glutamate in brain has long been suggested as the underlying pathophysiology of PDS. CSF glutamate concentration was elevated during the off- pyridoxine period in patient 3, but not in patient 2 or 5. These results suggest allelic and non-allelic heterogeneities of PDS, and that the CSF glutamate elevation does not directly correlate with the presence of *ALDH7A1* mutations.

Keywords: Vitamin B_6; Convulsion; ALDH7A1 gene; Pipecolic acid; Genetic heterogeneity; Private mutations; A large deletion; *Alu* repeats; Lymphoblasts; RT-PCR analysis

Pyridoxine dependent seizure (PDS) is a disorder of neonates or infants with autosomal recessive inheritance (MIM 266100) characterized by intractable seizures, which is responsive to administration of pharmacological dose of pyridoxine, but refractory to ordinary anticonvulsants [1,2]. The diagnosis as having PDS can be confirmed by

Abbreviations: PDS, pyridoxine-dependent seizures; GAD, glutamate decarboxylase; GABA, γ-amino butyric acid; CSF, cerebrospinal fluid; P6C, L-Δ^1-piperidine-6-carboxylate; PLP, pyridoxal phosphate; EEG, electroencephalogram; RT-PCR, reverse transcription-mediated PCR; PA, pipecolic acid.

* Corresponding author. Fax: +81 22 717 8142.
E-mail address: skure@mail.tains.tohoku.ac.jp (S. Kure).

1096-7192/$ - see front matter © 2007 Elsevier Inc. All rights reserved.
doi:10.1016/j.ymgme.2007.02.010

the withdrawn test of pyridoxine. In the case of PDS, seizures resume within 7–10 days. Patients with PDS are dependent on pharmacological dose of pyridoxine for the rest of their lives to remain seizure-free. Development delay is not rare, even with early diagnosis and treatment [3]. Linkage analysis of PDS families with multiple affected members has mapped a PDS gene on chromosome 5q31 [4]. Biochemical analysis has revealed that pipecolic acid concentration was elevated in plasma and CSF in PDS patients [5]. L-Pipecolic acid (PA) is converted by PA oxidase into L-Δ^1-piperidine-6-carboxylate (P6C). Accumulated P6C can bind and inactivate pyridoxal phosphate (PLP) *in vivo* by Knoevenagel condensations, which is supposed to cause depletion of intracellular PLP. Based on these biochemical findings, Mills et al., hypothesized that PDS has a lesion in P6C dehydrogenase encoded by ALDH7A1 gene on chromosome 5q31 [6]. They have successfully identified causative *ALDH7A* mutations in PDS families. Plecko et al have subsequently reported the *ALDH7A1* mutational analysis in 18 patients, and found that a missense mutation, E399Q, was most prevalent in Caucasian patients [7].

The purpose of this study is to elucidate further the genetic background of PDS by mutational analysis of PDS families, especially in Oriental patients. We screened *ALDH7A1* mutations in five PDS families, which included one family with elevated CSF glutamate level [8] and two families with normal CSF glutamate level [9,10] during pyridoxine-withdrawal period. The mutational analysis of the ALDH7A1 gene revealed complex etiological nature of PDS.

Methods

Subjects

We studied five apparently non-related patients, patients 1–5 (Table 1). All of the patients were products of parents with non-consanguineous marriage. Patient 4 had an affected younger sister while in the other families there was no history of affected siblings. Diagnosis as having PDS was confirmed by pyridoxine withdrawal test in all the patients. Profiles of patients 1–5 were summarized in Table 1, including onset of convulsive seizures, findings of electroencephalogram (EEG), status of psychomotor developments. This study was approved by Ethical Committee of Tohoku University School of Medicine.

Mutational analysis of the ALDH7A1 gene

Peripheral leukocyte DNA was obtained from patients and their parents. All of the 18 protein-coding exons in ALDH7A1 gene were amplified by PCR as described [6]. PCR products were size-separated on 2.5% agarose gel electrophoresis. Then the band with expected size was excised, purified, and subjected to direct sequencing analysis as described [11].

Reverse transcription-mediated PCR (RT-PCR)

Lymphoblast cell lines were established from blood samples from two control subjects and patients 4 and 5 by infection of Epstain–Barr virus. Total RNA was isolated from 5×10^6 cells of lymphoblast cells using RNeasy kit (Qiagen, Germany). Complementary DNA was synthesized from 10 μg of total RNA in a 20 μl mixture according to the manufacturer's instruction (Superscript II, Invitrogen, Carlsbad, Calif.). Subsequently, an entire coding region of *ALDH7A1* cDNA was amplified by three sets of PCR using 1 μl of the first-strand synthesis mixtures. The most 5′ part of cDNA with 504 bp in size containing exons 1–6 was amplified with forward primer (AASA-cDNA-5 F), 5′-TGTAAAACGACGGCCAGTTTGGAGCAGGCCTGCCGCCTTC-3′ and reverse primer (AASA-cDNA-5R), 5′-CAGGAAACAGCTATGACCCCAACCAGGCCTACGGGATTCC-3′. The middle part of cDNA (343 bp) corresponding to exons 6–9 was amplified with forward primer (AASA-cDNA-6F), 5′-TGTAAAACGACGGCCAGTTGGCCATGCACTGATTGAGCAGT-3′ and reverse primer (AASA-cDNA-6R), 5′-CAGGAAACAGCTATGACCCTCCTGCACCATCAGGCCCACC-3′. The most 3′ part fragment with 974 bp in size containing exons 8–18 was amplified with forward primer (AASA-cDNA-3F), 5′-TGTAAAACGACGGCCAGTGTTCCTTGACTTGTGGTGGAGC-3′ and reverse primer (AASA-cDNA-4R), 5′-CAGGAAACAGCTATGACCAATGCATTTATTCAGGGAAAACTT-3′. Singly and doubly underlined sequences were universal M13 and reverse sequences, respectively, for further sequencing analysis. Long range PCR was performed with LA-PCR kit (Takara Bio Inc., Tokyo, Japan). Primers for long-range PCR were forward primer, AASA-E16F, 5′-TGTAAAACGACGGCCAGTGGGGCTGAGATTGGAGGTGCC-3′ and reverse primer, AASA-cDNA-4R as mentioned above. The PCR products were size-separated by 1% agarose gel electrophoresis and visualized by ethidium bromide staining.

Multiplex RT-PCR analysis

A human β-actin cDNA with 1206 bp was co-amplified with the 3′ part of the *ALDH7A1* cDNA (974 bp) using Multiplex PCR kit (Qiagen, Germany). Nucleotide sequences of PCR primers for β-actin cDNA were reported previously [12]. The multiplex PCR products were subjected to 2.5% agarose gel electrophoresis. Intensity ratio of the two bands was measured by NIH image software for evaluation of *ALDH7A1* mRNA level.

Plasma PA concentration

Plasma samples were collected in patient 2, 4, and 5, and stored at −20 °C until analysis. Their PA concentrations were determined using gas chromatography mass spectrometry (GCMS-QP Model 2010, Shimadzu Biotech, Kyoto, Japan) as described [13,14].

Results

Sequencing analysis of ALDH7A1 genes

Sequencing analysis of entire coding regions of the ALDH7A1 gene in patients 1–4 revealed seven point mutations. In patient 1, two missense mutations were identified: G378R mutation in exon 14 and D449N mutation in exon 16 (Fig. 1a). In patient 2, P403L missense mutation was found in exon 14 in a heterozygous form. Additional single base substitution from A to T was observed at the splicing-donor site of intron 1, IVS1+3A>T (Fig. 1b). In patient 3, two missense mutations, G174V and V367G (Fig. 1c) were identified in exon 6 and exon 13, respectively, both of which have been reported [7]. In patient 4, a nonsense mutation (W31X) in exon 1 was found in the paternal allele, but no mutation was detected in the maternal allele by the sequencing analysis (Fig. 1d). Amino acid residues at these missense mutations, Gly^{174}, Val^{367}, Gly^{378}, Pro^{403}, and Asp^{449}, are highly conserved among vertebrae, higher plant, and bacteria, suggesting their evolutional importance. Any of the seven base substitutions described

Table 1
Profiles of patients with PDS

	Patient 1	Patient 2	Patient 3	Patient 4[a]	Patient 5
Ethnicity	Japanese	Japanese	German	Japanese	Japanese
Sex	Male	Male	Male	Male	Male
Consanguinity	(−)	(−)	(−)	(−)	(−)
Clinical findings at birth					
Gestational age (week)	38 weeks	39 weeks	—	40 weeks	37 weeks
Birth weight (g)	3000 g	3340 g	—	3400 g	3270 g
Apgar score at 5 min after delivery	10	NA[b]	10	NA	9
Onset of symptoms					
Onset of convulsion	2 days of life	2 h of life	3 weeks of age	2 days of life	18 days of life
Type of fit	Generalized tonic clonic	Generalized tonic clonic	Generalized tonic clonic	Generalized tonic clonic, myoclonic jerks	Focal seizures, occasionally generalized
Age at first trial of pyridoxine	4 day of life	5 months of age	3 months of age	4 month of age	19 days of life
Initial maintenance daily dose	16 mg/kg/day	13.5 mg/kg/day	24 mg/kg/day	11.8 mg/kg/day	30 mg/kg/day
Withdrawal test of pyridoxine					
Age at the test	6 months	7 months	5, 19, and 32 months	4 months	1 month
Type of convulsion	Tonic–clonic convulsion	Tonic–clonic convulsion	Tonic–clonic convulsion	Myoclonic jerks	Tonic convulasion
Delay before recurrence of seizures	3 days	6 days	10, 7, and 14 days, respectively	3 days	7 days
CSF glutamate concentration					
On the pyridoxine administration	NA	< 1.0 μM[c]	0.16 μM[d]	NA	1.16 μM
Off the pyridoxine administration	NA	< 1.0 M[c]	105.4 M[d]	NA	0.07 M
EEG finding					
Ictal	Hypsarrhythmia	Suppression burst	Hypsarrhythmia	Hypsarrhythmia	NA
Seizure- free period	Normal	Normal	Normal	Normal	Normal
MRI findings	NA	Moderate brain atrophy	No abnormal findings	NA	No abnormal findings
Development	Mild mental retardation	Mild mental retardation	Mild mental retardation	Mental retardation	Not retarded
ALDH7A1 mutational analysis					
Mutation 1	G378R (exon 14)	IVS1+3A>T (intron 1)	G174V (exon 6)	W31X (exon 1)	Not found
Mutation 2	D499N (exon 16)	P403L (exon 14)	V367G (exon 13)	1937- bp deletion (intron16–17)	Not found
Number of CA repeats in *ALDH7A1* intron 2	17/20	16/23	19/19	16/18	21/23
Plasma PA concentrations (μM)	NA	7.4	NA	7.2	4.6
Normal minimum–maximum values at the patient's age[e]	—	0.7–2.6	—	0.7–2.6	0.4–4.9
References	This study	Goto et al. [10]	Baumeister et al. [8] Plecko et al. [22]	Iinuma et al. [23]	This study

[a] His younger sister is also affected with PDS.
[b] NA, not available.
[c] CSF glutamate concentrations were determined as deswcribed [21].
[d] CSF glutamate concentrations were determined as deswcribed [9].
[e] Plecko et al., [7].

above was not found in 100 control alleles. No nucleotide change was found in patient 5.

A CA-repeat polymorphism in intron 2 of ALDH7A1 gene

We found that the CA repeat in most 5' part of intron 2 was highly polymorphic during sequencing analysis of exon 2. The repeat number of the CA was easily determined by sequencing analysis or polyacrylamide gel electrophoresis (data not shown). Repeat numbers of CA in patients 1–5 were shown in Table 1.

An ALDH7A1 deletion in family 4

Since the maternal mutation of patient 4 remained unidentified after the exon sequencing analysis, we studied *ALDH7A1* mRNA expressed in lymphoblasts of patient 4 by the RT-PCR method. Three sets of PCR were employed

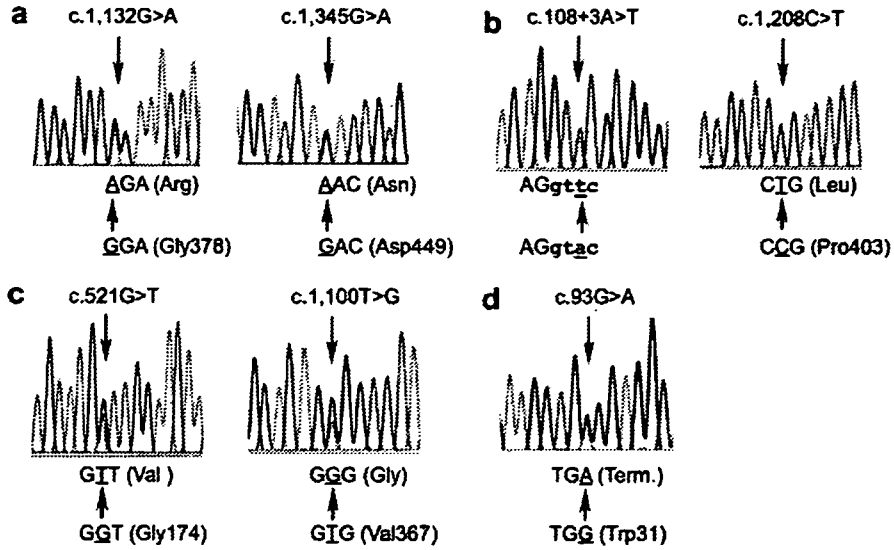

Fig. 1. Sequencing analysis of ALDH7A1 gene in patients 1–4. Sequencing chromatograms of each mutated nucleotide in patient 1 (a), patient 2 (b), patient 3 (c), and patient 4 (d) are shown. All the identified mutations were heterozygous. No mutations were found in patient 5.

for amplification of the *ALDH7A1* cDNA. Sequencing analysis of the most 5′ cDNA fragment (504 bp) and the middle part of the cDNA fragment (343 bp) revealed no sequence abnormality (data not shown). The most 3′ part of the control cDNA fragment, which contained exons 9–18, was 974 bp while the cDNA fragment of patient 4 was found to be smaller by 76 bp (Fig. 2a). Sequencing analysis of the smaller fragment revealed that the entire exon 17 was missing, suggesting a heterozygous deletion of exon 17. Subsequently, long-range PCR analysis was performed using primers AASA-E16F and AASA-cDNA-4R. A ~5 kb fragment was amplified in a control subject while an additional smaller band with ~3 kb was generated in patient 4, suggesting a heterozygous deletion of ~2 kb (Fig. 2b). Sequencing analysis of the 3-kb fragment revealed that a 1937-bp deletion that contained 3′ part of

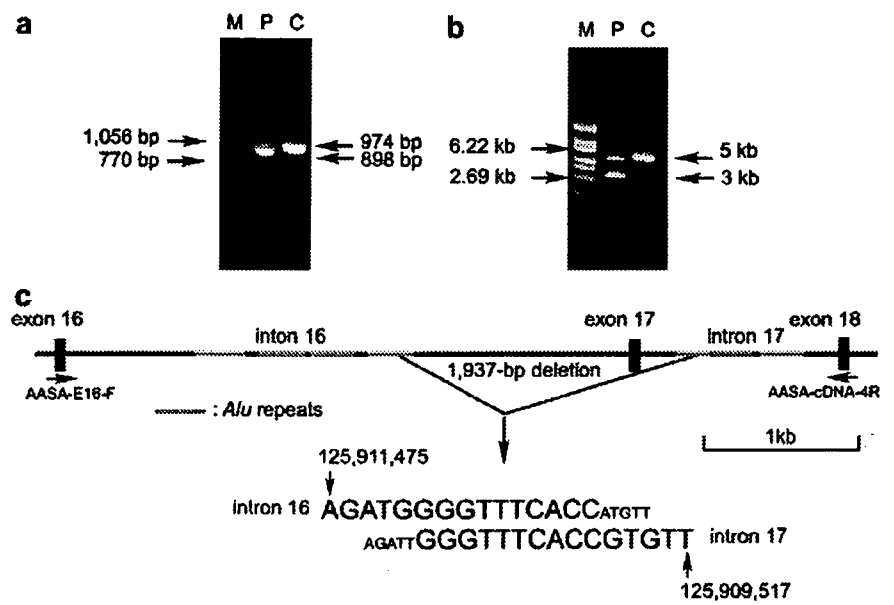

Fig. 2. An *ALDH7A1* genomic deletion in patient 4 (a) RT-PCR analysis of 3′ part of *ALDH7A1* cDNA in lymphoblasts from control and patient 4. The size of cDNA fragment was 76-bp shorter in patient 4 (lane P) than a control cDNA (lane C). Lane M represents DNA size marker. (b) Long-range PCR analysis using genomic DNA from a control subject (lane C) and patient 4 (lane P). PCR amplification in patient 4 yielded an additional smaller band (~3 kb). Locations of the PCR primers (AASA-E16F and AASA-cDNA-4R) were shown in panel C. (c) A schematic drawing of a 1937-bp deletion identified in patient 4. Gray short lines indicate *Alu* elements. Note that introns 16 and 17 have four and three copies of *Alu* elements, respectively, and that the deleted fragment was flanked by two *Alu* elements.

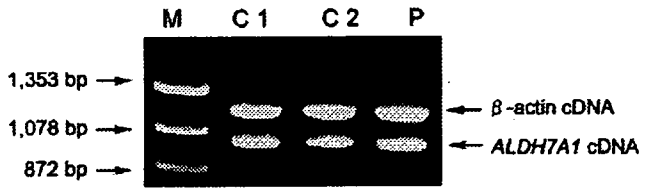

Fig. 3. Expression of ALDH mRNA in lymphoblasts from patient 5. A 1206-bp β-actin cDNA fragment and a 974-bp *ALDH7A1* cDNA fragment were simultaneously amplified by the multiplex PCR. Intensity ratio of the two cDNA fragments (ALDH7A1/β-actin) were measured. Lane M, DNA size marker; lane C1 and C2, control lymphoblast cDNA; lane P, lymphoblast cDNA of patient.

intron 16 (1478 bp), entire exon 17 (76 bp), and 5′ part of intron 17 (383 bp) as shown in Fig. 2c.

RT-PCR analysis of ALDH7A1 mRNA expressed in lymphoblasts of patient 5

Since the exon sequencing analysis revealed no causative alternations in patient 5, we analyzed the expression level of *ALDH7A1* mRNA by multiplex RT-PCR method. Human β-actin mRNA was used for an internal control of the mRNA level. The multiplex PCR yielded a 1206-bp fragment of β-actin cDNA and a 974-bp fragment of *ALDH7A1* cDNA (Fig. 3). Intensity ratio of the two cDNA bands (ALDH7A1/β-actin) was determined by NIH image. The ratios in control lymphoblasts 1, 2 and patient 5 were 0.86, 0.68, and 0.80, respectively, suggesting that *ALDH7A1* mRNA level in the lymphoblast of patient 5 was comparable with those in control lymphoblasts.

Plasma PA concentration

Plasma PA concentration of patients 2, 4, and 5 and the normal values at their ages [7] were shown in Table 1. The PA level was elevated to nearly threefold in patients 2 and 4 while it was within normal range in patient 5.

Discussion

We screened the *ALDH7A1* mutations in five non-consanguineous PDS patients, and found that patients 1–4 were compound heterozygotes of *ALDH7A1* mutations. Eight *ALDH7A1* mutations including six novel mutations were identified in this screening: five missense mutations, one nonsense mutation, one point mutation at the splicing donor site, and a 1937-bp genomic deletion. No founder mutations were identified in this study, which was in line with the highly heterogeneous result of the CA repeat polymorphism in intron 2 (Table 1). Since the repeat number is highly polymorphic it can be used for the allele transmission analysis. A missense mutation, E399Q, has been reported to be prevalent in Caucasian patients, accounting for 33% of the PDS mutant alleles [7]. In contrast, all the mutations identified in the current study were "private", found only in a single family, suggesting that *ALDH7A1* mutations in PDS are highly heterogeneous in the Oriental patients.

In patient 5, no mutation was identified in the coding regions of ALDH7A1 gene. Since the *ALDH7A1* mRNA expression level was not reduced in his lymphoblasts, compared with control subjects it is unlikely that an unidentified mutation resides in the promoter or enhancer regions of the ALDH7A1 gene. Sequencing analysis of the *ALDH7A1* cDNA revealed no structural abnormality, leaving little possibility of intronic mutations that cause aberrant splicing. Normal level of plasma PA in patient 5 also suggests that function of the ALDH7A1 gene is not impaired. It, therefore, appears unlikely that mutations in *ALDH7A1* caused PDS in patient 5. The diagnosis of patient 5 as having PDS was confirmed by pyridoxine withdrawal test at age of 26 days (Table 1). Bennett et al. previously reported one North American pedigree with PDS, in which the linkage with 5q13 was excluded by the linkage analysis [15]. Our study, together with the previous report, suggests the presence of another disease-causing gene for PDS other than *ALDH7A1*.

A 1937-bp *ALDH7A1*deletion was found in patient 4, which was suggested by a smaller cDNA fragment in the RT-PCR analysis. The RT-PCR generated no cDNA fragment with normal size (974 bp) despite the heterozygosity of the large deletion. It may be explained by non-sense mediated mRNA decay of the other allele with a nonsense mutation, W31X [16]. The deleted genomic fragment was flanked by two *Alu* elements in introns 16 and 18 (Fig. 2c), suggesting that the deletion was caused by *Alu*-mediated homologous recombination. In human genome, *Alu* repeats are distributed every ~4 kb in average [17]. Introns 16 and 17 of ALDH7A1 gene are rich in *Alu* elements: four copies in intron 16 with 3.5 kb and three copies in intron 17 with 1.3 kb. Heterozygous genomic deletions as seen in patient 4 cannot be detected by standard exon-sequencing analysis of ALDH7A1 gene. No mutation was identified by exon sequencing analysis in 2 of 36 PDS alleles in the previous study [7]. A large genomic deletion may remain unidentified in these mutant alleles. One should, therefore, consider an *ALDH7A1* genomic deletion, especially in the *Alu*-rich region like introns 15–17, when only one heterozygous mutation was identified by the exon-sequencing analysis.

It remains unknown how seizures develop by depletion of intracellular PLP in PDS. P6C is probably accumulated in by *ALDH7A1*mutations, which inactivates intracellular PLP *in vivo* [6]. It had long been proposed that PDS is caused by mutations in the genes that encodes glutamate decarboxylase (GAD), which generates an inhibitory neurotransmitter, γ-amino butyric acid (GABA) from an excitatory neurotransmitter, glutamate [18]. Dysfunction of GAD is supposed to result in accumulation of extracellular glutamate and/or depletion of extracellular GABA, which likely results in development of seizures. Genetic

involvement of either *GAD1* or *GAD2* was excluded by mutational analysis [19] and polymorphic marker analysis [20] of PDS families. Although genetic defects of GAD in PDS had been excluded it is still possible that enzymatic GAD activity is impaired by depletion of intracellular PLP. In our patients, CSF glutamate concentrations without pyridoxine administration were measured in patients 2, 3, and 5 (Table 1). CSF glutamate level was elevated in patient 3 [8] but not in patient 2 [10] or patient 5. Therefore, elevation of CSF glutamate level during off-pyridoxine period dose not directly correlated with the presence of *ALDH7A1* mutations. Other unknown factor(s) may participate in etiology of elevation of CSF glutamate. Further study is necessary for elucidation of the mechanism for seizure development by depletion of intracellular PLP.

Acknowledgements

We are grateful to the families who participated in this study. This work was supported by a grant from the Ministry of Education, Culture, Sports, Science, and Technology in Japan, and a grant from the Ministry of Health, Labor, and Public Welfare in Japan.

References

[1] A.D. Hunt Jr., J. Stokes Jr., C.W. Mc, H.H. Stroud, Pyridoxine dependency: report of a case of intractable convulsions in an infant controlled by pyridoxine, Pediatrics 13 (1954) 140–145.

[2] P. Baxter, P. Griffiths, T. Kelly, D. Gardner-Medwin, Pyridoxine-dependent seizures: demographic, clinical, MRI and psychometric features, and effect of dose on intelligence quotient, Dev. Med. Child Neurol. 38 (1996) 998–1006.

[3] S.M. Gospe, Pyridoxine-dependent seizures: findings from recent studies pose new questions, Pediatr. Neurol. 26 (2002) 181–185.

[4] V. Cormier-Daire, N. Dagoneau, R. Nabbout, L. Burglen, C. Penet, C. Soufflet, I. Desguerre, A. Munnich, O. Dulac, A gene for pyridoxine-dependent epilepsy maps to chromosome 5q31, Am. J. Hum. Genet. 67 (2000) 991–993.

[5] B. Plecko, S. Stockler-Ipsiroglu, E. Paschke, W. Erwa, E.A. Struys, C. Jakobs, Pipecolic acid elevation in plasma and cerebrospinal fluid of two patients with pyridoxine-dependent epilepsy, Ann. Neurol. 48 (2000) 121–125.

[6] P.B. Mills, E. Struys, C. Jakobs, B. Plecko, P. Baxter, M. Baumgartner, M.A. Willemsen, H. Omran, U. Tacke, B. Uhlenberg, B. Weschke, P.T. Clayton, Mutations in antiquitin in individuals with pyridoxine-dependent seizures, Nat. Med. 12 (2006) 307–309.

[7] B. Plecko, K. Paul, E. Paschke, S. Stoeckler-Ipsiroglu, E. Struys, C. Jakobs, H. Hartmann, T. Luecke, M. di Capua, C. Korenke, C. Hikel, E. Reutershahn, M. Freilinger, F. Baumeister, F. Bosch, W. Erwa, Biochemical and molecular characterization of 18 patients with pyridoxine-dependent epilepsy and mutations of the antiquitin (ALDH7A1) gene, Hum. Mutat. 28 (2007) 19–26.

[8] F.A. Baumeister, W. Gsell, Y.S. Shin, J. Egger, Glutamate in pyridoxine-dependent epilepsy: neurotoxic glutamate concentration in the cerebrospinal fluid and its normalization by pyridoxine, Pediatrics 94 (1994) 318–321.

[9] S. Kure, T. Maeda, N. Fukushima, T. Ohura, K. Takahashi, T. Nishikawa, Y. Matsubara, T. Izumi, K. Narisawa, A subtype of pyridoxine-dependent epilepsy with normal CSF glutamate concentration, J. Inherit Metab. Dis. 21 (1998) 431–432.

[10] T. Goto, N. Matsuo, T. Takahashi, CSF glutamate/GABA concentrations in pyridoxine-dependent seizures: etiology of pyridoxine-dependent seizures and the mechanisms of pyridoxine action in seizure control, Brain Dev. 23 (2001) 24–29.

[11] S. Kure, K. Kato, A. Dinopoulos, C. Gail, T.J. DeGrauw, J. Christodoulou, V. Bzduch, R. Kahmanchey, G. Fekete, A. Trojovsky, B. Plecko, G. Breningstall, J. Tohyama, Y. Aoki, Y. Matsubara, Comprehensive mutation analysis of GLDC, AMT, and GCSH in nonketotic hyperglycinemia, Hum. Mutat. 27 (2006) 343–352.

[12] M. Ogasawara, Y. Matsubara, H. Mikami, K. Narisawa, Identification of two novel mutations in the methylmalonyl-CoA mutase gene with decreased levels of mutant mRNA in methylmalonic acidemia, Hum. Mol. Genet. 3 (1994) 867–872.

[13] R.M. Kok, L. Kaster, A.P. de Jong, B. Poll-The, J.M. Saudubray, C. Jakobs, Stable isotope dilution analysis of pipecolic acid in cerebrospinal fluid, plasma, urine and amniotic fluid using electron capture negative ion mass fragmentography, Clin. Chim. Acta 168 (1987) 143–152.

[14] E.A. Struys, C. Jakobs, Enantiomeric analysis of D- and L-pipecolic acid in plasma using a chiral capillary gas chromatography column and mass fragmentography, J. Inherit. Metab. Dis. 22 (1999) 677–678.

[15] C.L. Bennett, H.M. Huynh, P.F. Chance, I.A. Glass, S.M. Gospe Jr., Genetic heterogeneity for autosomal recessive pyridoxine-dependent seizures, Neurogenetics 6 (2005) 143–149.

[16] E. Nagy, L.E. Maquat, A rule for termination-codon position within intron-containing genes: when nonsense affects RNA abundance, Trends Biochem. Sci. 23 (1998) 198–199.

[17] D.J. Rowold, R.J. Herrera, Alu elements and the human genome, Genetica 108 (2000) 57–72.

[18] K. Gibson, C. Jakobs, Disorders of β-and γ-amino acids in free and peptide-linked forms, in: C.R. Scriver, A.L. Beaudet, W.S. Sly, D. Valle (Eds.), The Metabolic and Molecular Bases of Inherited Disease, vol. 2, McGraw-Hill, New York, 2001, pp. 2079–2105.

[19] S. Kure, Y. Sakata, S. Miyabayashi, K. Takahashi, T. Shinka, Y. Matsubara, H. Hoshino, K. Narisawa, Mutation and polymorphic marker analyses of 65K- and 67K-glutamate decarboxylase genes in two families with pyridoxine-dependent epilepsy, J. Hum. Genet. 43 (1998) 128–131.

[20] G. Battaglioli, D.R. Rosen, S.M. Gospe Jr., D.L. Martin, Glutamate decarboxylase is not genetically linked to pyridoxine-dependent seizures, Neurology 55 (2000) 309–311.

[21] H. Iwama, K. Takahashi, S. Kure, F. Hayashi, K. Narisawa, K. Tada, M. Mizoguchi, S. Takashima, U. Tomita, T. Nishikawa, Depletion of cerebral D-serine in non-ketotic hyperglycinemia: possible involvement of glycine cleavage system in control of endogenous D-serine, Biochem. Biophys. Res. Commun. 231 (1997) 793–796.

[22] B. Plecko, C. Hikel, G.C. Korenke, B. Schmitt, M. Baumgartner, F. Baumeister, C. Jakobs, E. Struys, W. Erwa, S. Stockler-Ipsiroglu, Pipecolic acid as a diagnostic marker of pyridoxine-dependent epilepsy, Neuropediatrics 36 (2005) 200–205.

[23] K. Iinuma, K. Narisawa, N. Yamauchi, T. Yoshida, T. Mizuno, Pyridoxine dependent convulsion: effect of pyridoxine therapy on electroencephalograms, Tohoku J. Exp. Med. 105 (1971) 19–26.

Leukemia in Cardio-facio-cutaneous (CFC) Syndrome: A Patient With a Germline Mutation in *BRAF* Proto-oncogene

Yoshio Makita, MD, PhD, Yoko Narumi, MD,† Makoto Yoshida, MD,* Tetsuya Niihori, MD, PhD,† Shigeo Kure, MD,† Kenji Fujieda, MD, PhD,* Yoichi Matsubara, MD,†‡ and Yoko Aoki, MD, PhD†*

Summary: Cardio-facio-cutaneous (CFC) syndrome is a multiple congenital anomaly/mental retardation syndrome characterized by a distinctive facial appearance, ectodermal abnormalities, and heart defects. Clinically, it overlaps with both Noonan syndrome and Costello syndrome, which are caused by mutations in 2 genes that encode molecules of the RAS/MAPK (mitogen activated protein kinase) pathway (*PTPN11* and *HRAS*, respectively). Recently, mutations in *KRAS*, *BRAF*, and *MEK1/2* have been identified in patients with CFC syndrome. Somatic mutations in *KRAS* and *BRAF* have been identified in various tumors. In contrast, the association with malignancy has not been noticed in CFC syndrome. Here we report a 9-year-old boy diagnosed with CFC syndrome and acute lymphoblastic leukemia. Sequencing analysis of the entire coding region of *KRAS* and *BRAF* showed a de novo germline *BRAF* E501G (1502A→G) mutation. Molecular diagnosis and careful observations should be considered in children with CFC syndrome because they have germline mutations in proto-oncogenes and might develop malignancy.

Key Words: cardio-facio-cutaneous syndrome, KRAS, *BRAF*, RAS/MAPK, leukemia

(*J Pediatr Hematol Oncol* 2007;29:287–290)

Cardio-facio-cutaneous (CFC) syndrome is a multiple congenital anomaly/mental retardation syndrome characterized by heart defects, facial dysmorphism, ectodermal abnormalities, and mental retardation.[1,2] CFC syndrome has many clinical features in common with those with Noonan syndrome and Costello syndrome, which are caused by mutations of proto-oncogenes *PTPN11* and *HRAS*, respectively. Both genes encode molecules in the RAS/mitogen activated protein kinase (MAPK) signaling pathway.[3,4] It has been reported that patients with Noonan syndrome develop juvenile myelomonocytic leukemia, neuroblastoma, and rhabdomtosarcoma.[5] Predisposition to tumors, including neuroblastoma, rhabdomyosarcoma, and bladder carcinoma, has been reported in patients with Costello syndrome.[6] Tumor screening protocols have been proposed for these 2 syndromes.[6] In contrast, little attention has been paid for the development of tumors in patients with CFC syndrome.

Recently, we and others have identified germline mutations in *KRAS*, *BRAF*, and *MEK1/2* in individuals with CFC syndrome.[2,7] These genes encode molecules in the RAS-RAF-ERK pathway. Somatic mutations in *KRAS* and *BRAF* were identified in various tumors. *KRAS* mutations occurred frequently in lung, colon, and pancreatic cancer[8] and *BRAF* mutations have been frequently identified in malignant melanoma, colon cancer, and thyroid cancer.[9]

We herewith report a 9-year-old Japanese patient with CFC syndrome associated with acute lymphoblastic leukemia (ALL) in whom a *BRAF* mutation was identified. Our observations, together with literature reviews of previous cases, suggest the importance of careful observation for malignancy in CFC syndrome.

CASE REPORT

The propositus was a 9-year-old Japanese boy. He was the first son of unrelated healthy parents. At birth paternal age was 33 years and maternal age was 22 years. Delivery at 36 weeks was uncomplicated and birth weight of the patient was 3240 g (+1.8 SD), length 48.7 cm (+0.8 SD), and occipitofrontal head circumference 39.2 cm (+3.9 SD). At the age of 3 months, the following anomalies were noted (Fig. 1): sparse curly hair, macrocephaly, bitemporal constriction, hyperterolism,

Received for publication June 22, 2006; accepted February 28, 2007.
From the *Department of Pediatrics, Asahikawa Medical College, Asahikawa; †Department of Medical Genetics, Tohoku University School of Medicine; and ‡Tohoku University 21st Century COE Program "Comprehensive Research and Education Center for Planning of Drug Development and Clinical Evaluation," Sendai, Japan.
Supported by Grants-in-Aid from the Ministry of Education, Culture, Sports, Science and Technology of Japan and from the Ministry of Health, Labor, and Welfare of Japan.
The authors have no financial interest in the outcome of this report.
Reprints: Yoko Aoki, MD, PhD, Department of Medical Genetics, Tohoku University School of Medicine, 1-1 Seiryo-machi, Sendai 980-8574, Japan (e-mail: aokiy@mail.tains.tohoku.ac.jp).

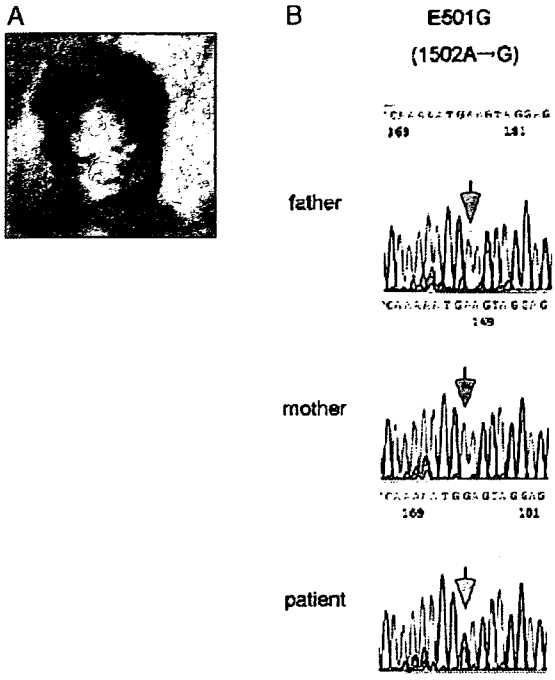

FIGURE 1. A, Facial appearance of the patient. B, The *BRAF* mutation in the patient, but not in his parents. The position of the nucleotide substitution is indicated by arrows.

downslanting palpebral fissures, low nasal bridge, low set and posterior rotated ears, bilateral cryptorchidism, generalized cutaneous pigmentation, and patchy hyperkeratosis, especially on extensor surfaces of limbs. Cardiac features included patent ductus arteriosus (naturally closed). At the age of 1 year and 3 months, asymmetrical hypertrophy of the interventricular septum directed toward the apex was noted. On the basis of the observed facial dysmorphisms, cardiac anomalies and skin abnormalities, he was diagnosed as having CFC syndrome.

He was diagnosed as having ALL at 1 year and 9 months of age, when his weight was 13.0 kg (+1.5 SD), his height was 88.0 cm (+1.3 SD) and his head circumference was 53 cm (+3.3 SD). He showed hepatosplenomegaly and right testicular swelling. Testicular involvement was confirmed by testicular biopsy. Lymphoblasts were seen in the peripheral blood (100% of 8.3×10^{10}/L leukocytes). Bone marrow aspirate showed 98% lymphoblasts positive for TdT, HLA-DR, CD19, CD10, CD22, and CD79a and negative for cytoplasmic IgM and membranous IgM, CD33, CD34, CD15, CD65, myeloperoxidase, and T-cell markers. Cytogenetic analysis of bone marrow aspiration was 46, XY (20 cells counts). The examination of cerebrospinal fluid showed no lymphoblasts.

Induction therapy, which consisted of vincristine, predonisolone, doxorubicin, and *Escherichia coli* asparaginase, was performed. Remission was achieved in 7 weeks. High-dose methotrexate and intrathecal therapy were performed for central nervous system prophylaxis. After induction treatment, right orchidodectomy was also performed. During maintenance therapy using vincristine, dexamethasone, 6-mercaptopurine, and methotrexate, a central nervous system relapse was observed at the age of 3 years and 9 months. Systemic investigation, including bone marrow aspiration, showed isolated central nervous system relapse. He received central nervous system irradiation (whole brain 24 Gy and whole spine 15 Gy, respectively). The maintenance therapy was finished at the age of 5 years and 9 months. Now, at the age of 9 years and 3 months, he is healthy except for severe mental retardation.

Mutation Analysis

Genomic DNA from blood leukocytes from the patient and the parents was isolated by a standard protocol. Five coding exons in *KRAS* and 18 coding exons in *BRAF* with flanked introns were amplified by polymerase chain reaction.[2,10] The polymerase chain reaction products were gel-purified and sequenced on an ABI PRISM 310 automated DNA sequencer (Applied Biosystems). This study was approved by the Ethics Committee of Tohoku University School of Medicine. We obtained informed consent for samples and specific consent for a photograph. Sequencing analysis of *BRAF* showed an A→G change at nucleotide 1502, resulting in an E501G mutation, in the heterozygous form[10] (Fig. 1B). The E501G mutation was not identified in DNA samples from his parents, suggesting that this mutation occurred de novo. No mutations were found in *KRAS*.

DISCUSSION

Germline mutations in *BRAF* have been found to account for 52% of patients with CFC syndrome.[2,7] A previous report has shown that a patient with CFC syndrome developed ALL at 5 years of age.[11] Later, a *BRAF* G469E mutation was identified in that patient (Table 1).[2] The type of leukemia was ALL of common phenotype. Chromosomal findings including TEL/AML1 fusion indicate a favorable ultimate outcome.[11] In the current study, we identified a de novo E501G mutation of *BRAF* in a CFC patient who developed ALL at 1 year and 9 months of age. Chromosomal abnormality of leukemia cells was not observed in the patient. Despite a central nervous system relapse and invasion of the testis by leukemia cells, induction and maintenance therapies were successful. *BRAF* is a proto-oncogene and somatic mutations in *BRAF* have been identified in 7% of cancer.[9] *BRAF* has been mutated in approximately 27% to 70% in malignant melanoma, 5% to 22% of the cases in colon cancer, and 36% to 53% of thyroid cancer.[9] The V600E mutation was frequently identified in these cancers. Somatic *BRAF* mutations have been also reported in 13 hematopoietic or lymphopoietic malignancies (The Sanger Institute Catalogue of Somatic Mutations in Cancer website). Careful observation and molecular analysis of patients can help clarify the predisposition to malignancy in CFC syndrome.

CFC syndrome shares clinical manifestations with Noonan syndrome and Costello syndrome. The clinical data of 19 mutation-positive CFC individuals showed a high frequency of growth failure (78.9%), mental retardation (100%), relative macrocephaly (78.9%), characteristic facial appearance including bitemporal constriction (84.2%) and downslanting palpebral fissures (94.7%), curly sparse hair (100%), heart defects (84.2%), and skin abnormalities (68.4%).[2] In contrast, Noonan syndrome has lower frequencies of mental retardation (24% to 35%), heart defects (50% to 67%), and skin

TABLE 1. Clinical Findings in CFC Patients Who Developed ALL

	Case 1[11]	Case 2 (Present Case)
Gene	*BRAF*	*BRAF*
Amino acid change	G469E	E501G
CFC		
Facial appearance	Typical	Typical
Heart defects	Mild PS, ASD, and asymmetrical hypertrophy of the interventricular septum	Patent ductus arteriosus and asymmetrical hypertrophy of the interventricular septum
Skin	Keratosis pilaris (3 y) cafe-au-lait spots	Generalized pigmentation and patchy hyperkeratosis
Other		Bilateral cryptorchidism
ALL		
Age at diagnosis	5 y	1 y 9 mo
Lymphoblasts in the peripheral blood	8% of 1.4×10^9/L leukocytes	100% of 8.3×10^{10}/L leukocytes
Lymphoblasts in bone marrow	98% lymphoblasts positive for TdT, HLA-DR, CD34, CD13, CD33, CD19, CD10, CD22, and CD79	98% lymphoblasts positive for TdT, HLA-DR, CD19, CD10, CD22, and CD79
Chromosomal abnormalities	45-46, XX, add(3)(p14), del(9) (p21p22), +10,t(12;21)(p13;22), +del(12)(p11;p12), del(15)(q13q24), der(16;19)(q10;p10), del(22)(q11q13)[27] and 46,XX[13] FISH studies were negative for BCR/ABL fusion and positive for TEL/AML1 fusion	46, XY. No visible structural anomaly was observed
Induction therapy	Vincristine, dexamethasone and *E. coli* asparginase	Vincristine, predonisolone, *E. coli* asparginase and doxorubicin
Central nervous system prophylaxis	Methotrexate	Methotrexate
Maintenance therapy	Vincristine, dexamethasone, 6-MP, and methotrexate	Vincristine, dexamethasone, 6-MP, and methotrexate
Central nervous system relapse	Absent	Present (during maintenance therapy)
Outcome	Unknown	Healthy as of age 9 y 3 mo
Other		Testicular involvement

ASD indicates atrial septal defect; PS, pulmonary stenosis.

abnormalities (2% to 27%).[12] Redundant skin (especially in the neck, hands, and feet), hypermobility of the small joints (especially in the fingers), and tightness of the Achilles tendons might be important clinical features to diagnose Costello syndrome.[4]

The risk of malignancy and types of tumors developed are different between these syndromes (Table 2). Past studies have shown that patients with Noonan syndrome develop leukemia, including juvenile myelomonocytic leukemia, neuroblastoma, or rhabdomyosarcoma.[5] Patients with Costello syndrome have been reported to develop various tumors, including rhabdomyosarcoma or neuroblastoma in the early infantile period and bladder carcinoma after 10 years of age.[6] Tumor frequency in Costello syndrome has been estimated to be as high as 17% and tumor screening protocol has been proposed.[6] The association with ALL was reported in 2 CFC patients with *BRAF* mutations including this report. Molecular diagnosis will lead to correct diagnosis of patients who are suspected of having Noonan-related syndromes and will be useful to determine the screening plan for malignancy in patients.

URL. The Sanger Institute Catalogue of Somatic Mutations in Cancer website is at http://www.sanger.ac.uk/cosmic.

TABLE 2. Noonan, Costello, and CFC Syndromes and Associated Tumors

Disease	Cancer	References
Noonan syndrome	Rhabdomyosarcoma	13, 14
	Subcutaneus granular-cell tumors	15
	Neuroblastoma	16–18
	Juvenile myelomonocytic leukemia	19–24
	Myeloproliferative disorder	24–27
	ALL	28
Costello syndrome	Rhabdomyosarcoma	4, 6, 29–31
	Neuroblastoma	4, 32
	Bladder carcinoma	33, 34
CFC syndrome	ALL	11, this study
	Rhabdomyosarcoma	35

ACKNOWLEDGMENT

The authors thank the family who participated in this study.

REFERENCES

1. Reynolds JF, Neri G, Herrmann JP, et al. New multiple congenital anomalies/mental retardation syndrome with cardio-facio-cutaneous involvement—the CFC syndrome. *Am J Med Genet*. 1986;25: 413–427.
2. Niihori T, Aoki Y, Narumi Y, et al. Germline KRAS and BRAF mutations in cardio-facio-cutaneous syndrome. *Nat Genet*. 2006;38: 294–296.

3. Tartaglia M, Mehler EL, Goldberg R, et al. Mutations in PTPN11, encoding the protein tyrosine phosphatase SHP-2, cause Noonan syndrome. *Nat Genet.* 2001;29:465–468.
4. Aoki Y, Niihori T, Kawame H, et al. Germline mutations in HRAS proto-oncogene cause Costello syndrome. *Nat Genet.* 2005;37: 1038–1040.
5. Tartaglia M, Gelb BD. Germ-line and somatic PTPN11 mutations in human disease. *Eur J Med Genet.* 2005;48:81–96.
6. Gripp KW, Scott CI Jr, Nicholson L, et al. Five additional Costello syndrome patients with rhabdomyosarcoma: proposal for a tumor screening protocol. *Am J Med Genet.* 2002;108:80–87.
7. Rodriguez-Viciana P, Tetsu O, Tidyman WE, et al. Germline mutations in genes within the MAPK pathway cause cardio-facio-cutaneous syndrome. *Science.* 2006;311:1287–1290.
8. Malumbres M, Barbacid M. RAS oncogenes: the first 30 years. *Nat Rev Cancer.* 2003;3:459–65.
9. Garnett MJ, Marais R. Guilty as charged: B-RAF is a human oncogene. *Cancer Cell.* 2004;6:313–319.
10. Narumi Y, Aoki Y, Niihori T, et al. Molecular and clinical characterization of cardio-facio-cutaneous (CFC) syndrome: overlapping clinical manifestations with Costello syndrome. *Am J Med Genet.* 2007;143:799–807.
11. van Den Berg H, Hennekam RC. Acute lymphoblastic leukaemia in a patient with cardiofaciocutaneous syndrome. *J Med Genet.* 1999; 36:799–800.
12. Wieczorek D, Majewski F, Gillessen-Kaesbach G. Cardio-facio-cutaneous (CFC) syndrome–a distinct entity? Report of three patients demonstrating the diagnostic difficulties in delineation of CFC syndrome. *Clin Genet.* 1997;52:37–46.
13. Khan S, McDowell H, Upadhyaya M, et al. Vaginal rhabdomyosarcoma in a patient with Noonan syndrome. *J Med Genet.* 1995; 32:743–745.
14. Jung A, Bechthold S, Pfluger T, et al. Orbital rhabdomyosarcoma in Noonan syndrome. *J Pediatr Hematol Oncol.* 2003;25:330–332.
15. Lohmann DR, Gillessen-Kaesbach G. Multiple subcutaneous granular-cell tumours in a patient with Noonan syndrome. *Clin Dysmorphol.* 2000;9:301–302.
16. Lopez-Miranda B, Westra SJ, Yazdani S, et al. Noonan syndrome associated with neuroblastoma: a case report. *Pediatr Radiol.* 1997; 27:324–326.
17. Ijiri R, Tanaka Y, Keisuke K, et al. A case of Noonan's syndrome with possible associated neuroblastoma. *Pediatr Radiol.* 2000; 30:432–433.
18. Cotton JL, Williams RG. Noonan syndrome and neuroblastoma. *Arch Pediatr Adolesc Med.* 1995;149:1280–1281.
19. Choong K, Freedman MH, Chitayat D, et al. Juvenile myelomonocytic leukemia and Noonan syndrome. *J Pediatr Hematol Oncol.* 1999;21:523–527.
20. Fukuda M, Horibe K, Miyajima Y, et al. Spontaneous remission of juvenile chronic myelomonocytic leukemia in an infant with Noonan syndrome. *J Pediatr Hematol Oncol.* 1997;19:177–179.
21. Yoshida R, Miyata M, Nagai T, et al. A 3-bp deletion mutation of PTPN11 in an infant with severe Noonan syndrome including hydrops fetalis and juvenile myelomonocytic leukemia. *Am J Med Genet A.* 2004;128:63–66.
22. Niihori T, Aoki Y, Ohashi H, et al. Functional analysis of PTPN11/SHP-2 mutants identified in Noonan syndrome and childhood leukemia. *J Hum Genet.* 2005;50:192–202.
23. Tartaglia M, Niemeyer CM, Fragale A, et al. Somatic mutations in PTPN11 in juvenile myelomonocytic leukemia, myelodysplastic syndromes and acute myeloid leukemia. *Nat Genet.* 2003;34: 148–150.
24. Kratz CP, Niemeyer CM, Castleberry RP, et al. The mutational spectrum of PTPN11 in juvenile myelomonocytic leukemia and Noonan syndrome/myeloproliferative disease. *Blood.* 2005;106: 2183–2185.
25. Bader-Meunier B, Tchernia G, Mielot F, et al. Occurrence of myeloproliferative disorder in patients with Noonan syndrome. *J Pediatr.* 1997;130:885–889.
26. Kratz CP, Nathrath M, Freisinger P, et al. Lethal proliferation of erythroid precursors in a neonate with a germline PTPN11 mutation. *Eur J Pediatr.* 2006;165:182–185.
27. Wilcox WD. Occurrence of myeloproliferative disorder in patients with Noonan syndrome. *J Pediatr.* 1998;132:189–190.
28. Attard-Montalto SP, Kingston JE, Eden T. Noonan's syndrome and acute lymphoblastic leukaemia. *Med Pediatr Oncol.* 1994;23: 391–392.
29. O'Neal JP, Ramdas J, Wood WE, et al. Parameningeal rhabdomyosarcoma in a patient with Costello syndrome. *J Pediatr Hematol Oncol.* 2004;26:389–392.
30. Sigaudy S, Vittu G, David A, et al. Costello syndrome: report of six patients including one with an embryonal rhabdomyosarcoma. *Eur J Pediatr.* 2000;159:139–142.
31. Feingold M. Costello syndrome and rhabdomyosarcoma. *J Med Genet.* 1999;36:582–583.
32. Moroni I, Bedeschi F, Luksch R, et al. Costello syndrome: a cancer predisposing syndrome? *Clin Dysmorphol.* 2000;9:265–268.
33. Franceschini P, Licata D, Di Cara G, et al. Bladder carcinoma in Costello syndrome: report on a patient born to consanguineous parents and review. *Am J Med Genet.* 1999;86:174–179.
34. Gripp KW, Scott CI Jr, Nicholson L, et al. Second case of bladder carcinoma in a patient with Costello syndrome. *Am J Med Genet.* 2000;90:256–259.
35. Bisogno G, Murgia A, Mammi I, et al. Rhabdomyosarcoma in a patient with cardio-facio-cutaneous syndrome. *J Pediatr Hematol Oncol.* 1999;21:424–427.

ELECTRONIC LETTER

Genomic deletion within *GLDC* is a major cause of non-ketotic hyperglycinaemia

Junko Kanno, Tim Hutchin, Fumiaki Kamada, Ayumi Narisawa, Yoko Aoki, Yoichi Matsubara, Shigeo Kure

J Med Genet 2007;44:e69 (http://www.jmedgenet.com/cgi/content/full/44/3/e69). doi: 10.1136/jmg.2006.043448

Background: Non-ketotic hyperglycinaemia (NKH) is an inborn error of metabolism characterised by accumulation of glycine in body fluids and various neurological symptoms. NKH is caused by deficiency of the glycine cleavage multienzyme system with three specific components encoded by *GLDC*, *AMT* and *GCSH*. Most patients are deficient of the enzymatic activity of glycine decarboxylase, which is encoded by *GLDC*. Our recent study has suggested that there are a considerable number of *GLDC* mutations which are not identified by the standard exon-sequencing method.

Methods: A screening system for *GLDC* deletions by multiplex ligation-dependent probe amplification (MLPA) has been developed. Two distinct cohorts of patients with typical NKH were screened by this method: the first cohort consisted of 45 families with no identified *AMT* or *GCSH* mutations, and the second cohort was comprised of 20 patients from the UK who were not prescreened for *AMT* mutations.

Results: *GLDC* deletions were identified in 16 of 90 alleles (18%) in the first cohort and in 9 of 40 alleles (22.5%) in the second cohort. 14 different types of deletions of various lengths were identified, including one allele where all 25 exons were missing. Flanking sequences of interstitial deletions in five patients were determined, and *Alu*-mediated recombination was identified in three of five patients.

Conclusions: *GLDC* deletions are a significant cause of NKH, and the MLPA analysis is a valuable first-line screening for NKH genetic testing.

Non-ketotic hyperglycinaemia (NKH), also called glycine encephalopathy, is an inborn error of glycine metabolism caused by deficiency of the glycine cleavage system (GCS).[1–3] Classically, NKH presents in the first few days of life with progressive lethargy, hypotonia, myoclonic jerks, hiccups and apnoea, usually leading to coma and death unless the patient is treated adequately.[4] Patients with atypical glycine encephalopathy often lack neonatal symptoms, but manifest aggressive behaviour, cognitive impairment, and impaired work or school performance.[5 6] Atypical patients manifest only non-specific clinical symptoms with most patients remaining undiagnosed and thus without the benefit of early diagnosis and treatment.[7] The fundamental defect of NKH lies in the mitochondrial GCS (EC2.1.2.10)[8] that consists of four individual proteins:[9] glycine decarboxylase encoded (also called P-protein) by *GLDC*; aminomethyltransferase (T-protein) encoded by *AMT*; hydrogen carrier protein (H-protein) encoded by *GCSH*; and dihydrolipoamide dehydrogenase encoded by *GCSL*. Dihydrolipoamide dehydrogenase is a housekeeping enzyme that serves as an E3 component of other enzyme complexes such as pyruvate dehydrogenase. The three GCS-specific genes are mapped on different chromosomes: *GLDC* on chromosome 9p24,[10] *AMT* on 3p21.1–21.2[11] and *GCSH* on 16q24.[12] Enzymatic analysis has shown that approximately 80% of patients with NKH are deficient of glycine decarboxylase activity.[13]

In Finnish patients we reported a common missense mutation, S564L that accounts for 70% of mutant alleles.[14] Toone *et al*[15] reported a missense mutation, R515S, in 5% of Caucasian mutant alleles. Most of the reported mutations are, however, private, found in only a single family,[16–20] thus making DNA analysis difficult. Recently, we have undertaken a comprehensive mutation screening of the three genes, *GLDC*, *AMT* and *GCSH*, in patients with neonatal, infantile and late-onset types of NHK.[21] Various *GLDC* and *AMT* mutations were identified in patients with neonatal and infantile types of NHK, but not in those with the late onset type. Among 56 patients with the neonatal type, *GLDC* mutations were found in 36 patients, whereas *AMT* mutations were identified in 11 patients. In 14 of 36 patients, *GLDC* mutations were identified in only one allele, suggesting that some mutations are not detected by the exon-sequencing method. We have reported several patients with deletion of *GLDC* exon 1,[22] and Sellner *et al*[20] have reported a patient with deletion of the *GLDC* exons 2–15. These studies suggest that a considerable number of deletions may remain unidentified in *GLDC*.

The purpose of the present study was to establish a method of screening for deletions within *GLDC* and determine their frequency in patients with NKH. A multiplex ligation-dependent probe amplification (MLPA) method[23] was used to screen 65 patients with NKH. Using this method, 14 different types of exonic deletions were found in 25 of 130 alleles (19%) in patients with NKH. Our results suggest that deletions in the *GLDC* gene are a common cause of NKH, and that MLPA analysis is a useful first-line screening in NKH genetic testing.

METHODS

Patients with NKH

DNA samples were obtained from two cohorts of patients with typical NKH with a neonatal onset. Our original cohort of 56 patients with neonatal-type NKH[21] was found to contain 11 patients with *AMT* mutations. We excluded those 11 patients and defined a new cohort of the remaining 45 patients with NKH (the *AMT*-mutation negative cohort). The second cohort contained 20 patients (14 Caucasian and 6 from the Indian subcontinent) with neonatal-type NKH, who were referred to the Birmingham Children's Hospital, Birmingham, UK, for enzymatic and genetic confirmation of the clinical diagnosis of NKH. In the second cohort, screening for only the R515S and

Abbreviations: GCS, glycine cleavage system; MLPA, multiplex ligation-dependent probe amplification; NKH, non-ketotic hyperglycinaemia; PCR, polymerase chain reaction; SNP, single-nucleotide polymorphism

Table 1 Multiplex ligation-dependent probe amplification probes and polymerase chain reaction products in control participants

Target		Upstream probe			Downstream probe			PCR product size (bp)	Control values (n=18)		
Gene	Exon	Name	Location	Length (base)	Name	Location	Length (base)		Peak area (mean (SD) arbitrary unit)	Relative peak area (mean (SD))*	SD/mean (%)
GLDC	Exon 1	M-GLDC-E1U	Exon 1	50	M-GLDC-E1D	Intron 1	50	100	26557 (1944)	11.52 (0.57)	5
	Exon 2	M-GLDC-E2U	Exon 2	54	M-GLDC-E2D	Intron 2	54	108	41534 (1673)	18.04 (0.47)	3
	Exon 3	M-GLDC-E3U	Exon 3	58	M-GLDC-E3D	Intron 3	58	116	44796 (1710)	19.46 (0.31)	2
	Exon 4	M-GLDC-E4U	Exon 4	62	M-GLDC-E4D	Intron 4	62	124	36206 (1216)	15.72 (0.42)	3
	Exon 5	M-GLDC-E5U-2	Intron 4	66	M-GLDC-E5D-2	Exon 5	66	132	43086 (2700)	18.72 (1.07)	6
	Exon 6	M-GLDC-E6U	Exon 6	70	M-GLDC-E6D	Intron 6	70	140	42903 (1261)	18.64 (0.30)	2
	Exon 7	M-GLDC-E7U	Exon 7	74	M-GLDC-E7D	Intron 7	74	148	36397 (1739)	15.80 (0.33)	2
	Exon 8	M-GLDC-E8U	Exon 8	78	M-GLDC-E8D	Intron 8	78	156	26102 (643)	11.34 (0.71)	6
	Exon 9	M-GLDC-E9U	Exon 9	80	M-GLDC-E9D	Intron 9	80	164	30208 (1499)	13.15 (0.37)	3
	Exon 10	M-GLDC-E10U	Exon 10	92	M-GLDC-E10D	Intron 10	80	172	19567 (1174)	8.49 (0.23)	3
	Exon 11	M-GLDC-E11U	Exon 11	100	M-GLDC-E11D	Intron 11	80	180	24892 (1987)	10.80 (0.61)	6
	Exon 12	M-GLDC-E12U	Exon 12	108	M-GLDC-E12D	Intron 12	80	188	16334 (949)	7.09 (0.21)	3
	Exon 13	M-GLDC-E13U-2	Exon 13	112	M-GLDC-E13D	Intron 13	80	192	23856 (1097)	10.36 (0.26)	2
	Exon 15	M-GLDC-E15U	Exon 15	52	M-GLDC-E15D	Intron 15	52	104	45980 (1888)	19.97 (0.54)	3
	Exon 16	M-GLDC-E16U	Exon 16	56	M-GLDC-E16D	Intron 16	56	112	40630 (1275)	17.66 (0.53)	3
	Exon 17	M-GLDC-E17U	Exon 17	60	M-GLDC-E17D	Intron 17	60	120	43310 (1651)	18.82 (0.57)	3
	Exon 18	M-GLDC-E18U-2	Intron 17	64	M-GLDC-E18D-2	Exon 18	64	128	20771 (1002)	9.02 (0.31)	3
	Exon 19	M-GLDC-E19U	Exon 19	68	M-GLDC-E19D	Intron 19	68	136	33246 (1049)	14.45 (0.28)	2
	Exon 20	M-GLDC-E20U	Exon 20	72	M-GLDC-E20D	Intron 20	72	144	27145 (1199)	11.79 (0.32)	3
	Exon 21	M-GLDC-E21U	Exon 21	76	M-GLDC-E21D	Intron 21	76	152	26832 (1246)	11.65 (0.24)	2
	Exon 22	M-GLDC-E22U	Exon 22	80	M-GLDC-E22D	Intron 22	80	160	23008 (1083)	10.00 (0.51)	5
	Exon 23	M-GLDC-E23U	Exon 23	88	M-GLDC-E23D	Intron 23	80	168	20373 (1428)	8.86 (0.38)	4
	Exon 24	M-GLDC-E24U-2	Intron 24	96	M-GLDC-E24D-2	Exon 24	80	176	20051 (609)	8.72 (0.31)	4
	Exon 25	M-GLDC-E25U	Exon 25	104	M-GLDC-E25D	Intron 25	80	184	29957 (1235)	13.10 (0.25)	2
	Processed pseudogene	M-GLDC-E1Ut	Pseudogene	50	M-GLDCP-1D	Pseudogene	47	97	33495 (1483)	–	–
EXT2	Exon 13	M-EXT2-E13U	Exon 13	41	M-EXT2-E13D	Exon 13	44	85	67822 (4013)	–	–
AMT	Exon 1	M-AMT-E1U	Exon 1	44	M-AMT-E1D	Intron 1	44	88	31455 (2656)	–	–
	Exon 4	M-AMT-E4U	Exon 4	45	M-AMT-E4D	Intron 4	46	91	27010 (1212)	–	–
	Exon 9	M-AMT-E9U-2	Intron 8	47	M-AMT-E9D-2	Exon 9	47	94	50490 (2102)	–	–

PCR, polymerase chain reaction.
*Peak area of each *GLDC* exon/sum of peak areas of *GLDCP*, *EXT2*, *AMT* exon 1, *AMT* exon 4 and *AMT* exon 9; †shared with upstream primer for *GLDC* exon 1.

Table 2 Nucleotide sequences of the MPLA probes for detection of *GLDC* deletions

Target gene	Probe name	Nucleotide sequences (5′ to 3′)
GLDC	M-GLDC-E1U	GGGTTCCCTAAGGGTTGGAGAGAGAGATGCTGCAGACCTTCGGGCTCGCG
	M-GLDC-E1D	*GTAAGGACCTCCACCCGGCCCTCCGCGTCTAGATTGGATCTTGCTGGCAC
	M-GLDC-E2U	GGGTTCCCTAAGGGTTGGATTTGAAAAGACCCTTGAAAATGGAAGACCCTGTTT
	M-GLDC-E2D	*GTAAGTGCCCCGCGACGGCTCCCTTGGACTTATCTAGATTGGATCTTGCTGGCAC
	M-GLDC-E3U	GGGTTCCCTAAGGGTTGGAACAGACGATTTTGCCGGAACTTACTGGAGAACTCAGGATG
	M-GLDC-E3D	*GTAATGTATTTCTCAGTTCAGGAACAGGATGACTGTCTAGATTGGATCTTGCTGGCAC
	M-GLDC-E4U	GGGTTCCCTAAGGGTTGGAATGAGGGCACTGCAGCCGCAGAGGCACTGCAGCTGTGCTACAG
	M-GLDC-E4D	*GTGAGAGCCCTCTCAAAGTGCTGGAATTCCAGTTGTGGGTCTAGATTGGATCTTGCTGGCAC
	M-GLDC-E5U-2	GGGTTCCCTAAGGGTTGGACTATTTATTTAATGTTCACGTTGGAATGTGCTTTTTCTTTTCAACAG
	M-GLDC-E5D-2	*ACACAACAAGAGGAGGCAAATTTCTCGTTGATCCCCGTTGCCACTCTAGATTGGATCTTGCTGGCAC
	M-GLDC-E6U	GGGTTCCCTAAGGGTTGGAGGGAAGGTGGAAGACTTTACGGAACTCGTGCAGAGAGCTCATCAGAGTGGG
	M-GLDC-E6D	*GTAGGTATACCTTTCTTGTGGGGGGTCCGTGGAGGCGTATCCCAACTTCTAGATTGGATCTTGCTGGCAC
	M-GLDC-E7U	GGGTTCCCTAAGGGTTGGACTGTCCGAGAAAGCTTGGTGAGAATGATGCCTGGAAGAATGGTCGCGGGTAACAAG
	M-GLDC-E7D	*GTAAAGGGGCTCATGTTTCTCTACTTTTATTGTGATTATGATTTCCCTGATTCTAGATTGGATCTTGCTGGCAC
	M-GLDC-E8U-2	GGGTTCCCTAAGGGTTGGACCATTTTCTCAGTGGGAACTAAGGGCGGCGCCTCTTCAGTTCCCAC
	M-GLDC-E8D-2	*CTGAGCATTCATATTTGCCCCGTCTAGGTAGACCTGTCCTCTCTAGATTGGATCTTGCTGGCAC
	M-GLDC-E9U	GGGTTCCCTAAGGGTTGGAATGTTCCCATGGGCTGGAGCATATTGCTACGACGGTACATAATGCCACTTTGATTTTGTCAGAAG
	M-GLDC-E9D	*GTGAGTTGGTAATCTGTCTAAAACATTTGGGCATAATAAAATTGATAAATTTGAGTATCTAGATTGGATCTTGCTGGCAC
	M-GLDC-E10U	GGGTTCCCTAAGGGTTGGAGCTGCTAGTGAAGGAGGTCTTGGGCAGGGCCGCTCAGCGGCAGATCAATTTTCGGCTTTT GACGATGGCACA
	M-GLDC-E10D	*GTAAGTCAAATTTTCAGTATTTTTACCAGTTTTTCAAATTTTCACATTGTTTCTCATTCTAGATTGGATCTTGCTGGCAC
	M-GLDC-E11U	GGGTTCCCTAAGGGTTGGACTTGGTATTTCTCTTGATGAGACAGTCAATGAAAAAGATCTGGACGATTTGTTGTGGATCTTTGG TTGTGAGTCATCTGCA
	M-GLDC-E11D	*GTAAGTAAAATAAAAACATGCGTTCCTCATCATAACTATTGGAGGTGGTAGCAAAAGTCTAGATTGGATCTTGCTGGCAC
	M-GLDC-E12U	GGGTTCCCTAAGGGTTGGAGCTGAAAGCATGGGAGAGGAGTGCAGAGGTATTCCACGGGTCTGTGTTCAAGAGGACC AGCCCGTTCCTCACCCATCAAGTGTTCAACAG
	M-GLDC-E12D	*GTTTGTGTGTCTTGTGTGACTTCTGCGTTTTGTGCTTTGGTAATCAGCTAGGGAGTTTCTAGATTGGATCTTGCTGGCAC
	M-GLDC-E13U-2	GGGTTCCCTAAGGGTTGGATGTTCACAGCTACCACTCTGAAACAAACATTGTCCGGTACATGAAGAAACTGGAAAATAAAGA CATTTCCCTTGTTCACAGCATGATTCCACT
	M-GLDC-E13D	*GGTAGTTATTTGTGGCCTTTTTTCTCATTTCCAAGCTACCCCAATCCCACGTCTCTTTCTAGATTGGATCTTGCTGGCAC
	M-GLDC-E15U	GGGTTCCCTAAGGGTTGGAAGGTTATGACCAGGTCTGTTTCCAGCCAAACAG
	M-GLDC-E15D	*CTAAGGGCATTTCTTTTCTTATTGTTTCATCTAGATTGGATCTTGCTGGCAC
	M-GLDC-E16U	GGGTTCCCTAAGGGTTGGAAGCCTACTTAAACCAGAAAGGAGAGGCGCACAGAAGG
	M-GLDC-E16D	*GTGAGTATGGCAGGAGGTGGCGCTTGCTCACCATCTAGATTGGATCTTGCTGGCAC
	M-GLDC-E17U	GGGTTCCCTAAGGGTTGGAATAAATATGGGAATATCGATGCAGTTCACCTCAAGGCCATG
	M-GLDC-E17D	*GTACTTGTCTTCCTCCTAGCAGATGGGAGAGGCCGGATCTAGATTGGATCTTGCTGGCAC
	M-GLDC-E18U-2	GGGTTCCCTAAGGGTTGGACCATTTTCTCAGTGGGAACTAAGGGCGGCGCCTCTTCAGTTCCCAC
	M-GLDC-E18D-2	*CTGAGCATTCATATTTGCCCCGTCTAGGTAGACCTGTCCTCTCTAGATTGGATCTTGCTGGCAC
	M-GLDC-E19U	GGGTTCCCTAAGGGTTGGATCTGCATTCCCCACGGAGGAGGTGGTCCTGGCATGGGGCCCCATCGGAGT
	M-GLDC-E19D	*GTAAGTTCTGGGCTGCTGGTTTCAGGATGGCTTTGGAGACAGAATTCTAGATTGGATCTTGCTGGCAC
	M-GLDC-E20U	GGGTTCCCTAAGGGTTGGACGGCCCCATGGGGCTCCAGTTCCATCTGCCCATTCCTGGGCTATATCAAG
	M-GLDC-E20D	*GTGACGCCTGGGAGTATGTGCAGGTGTGCAGGTGGGTGGGGGCGTCAGGTCTAGATTGGATCTTGCTGGCAC
	M-GLDC-E21U	GGGTTCCCTAAGGGTTGGAACTACATGGCCAAGCGATTAGAAACACACTACAGAATTCTTTCAGGGGTGCAAGAG
	M-GLDC-E21D	*GCAAGTATCAACTTAATCTATCATTACTTGGTTTTTTTCTTGGCCAAACTAATCTAGATTGGATCTTGCTGGCAC
	M-GLDC-E22U	GGGTTCCCTAAGGGTTGGACCCTTCAAAAAGTCTGCAAATATTGAGGCTGTGGATGTGGCCAAGAGACTCCAGGATTATG
	M-GLDC-E22D	*GTAAGTGGCTTTGACATTCATGCCGCCGCCCATGCTGGCTGTGGACCACTTCCTAATCTAGATTGGATCTTGCTGGCAC
	M-GLDC-E23U	GGGTTCCCTAAGGGTTGGAATCAGCATTCGGCAGGAAATTGCTGACATTGAGGAGGGCCGCATCGACCCCAGGGTCAAT CCGCTGAAG
	M-GLDC-E23D	*GTGCGTAGGCCCTGGAACATTGCTTGAAATGTTCCTTAAACTAGAAAATGATGTCTGTCTAGATTGGATCTTGCTGGCAC
	M-GLDC-E24U-2	GGGTTCCCTAAGGGTTGGAGCTAAGAGCGTACACCCGTCAGGATAGGAGCTGGCCCATGCCTTCCCAGCTGGCACATTC AGATTCAGAGAACTTAC
	M-GLDC-E24D-2	*GAGTGGGAATGCTGCCACCTCTCTGGAATAAGGCCGGTCCCAGTGGGAAGATGTAACTCTAGATTGGATCTTGCTGGCAC
	M-GLDC-E25U	GGGTTCCCTAAGGGTTGGATGTGGGACTAGCATTGCCACCTCCTTTGCCCTAAGAGAAACCCTCCCAGAACATCTCACACCA TTTCCATCTTTGTCCTTTGCAG
	M-GLDC-E25D	*CCCTTCGTGAAACCAGAGAACAAATTCTGGCCAACGATTGCCCGGATTGATGACATATCTAGATTGGATCTTGCTGGCAC
GLDCP	M-GLDCP-1D	*AGCATTGATGAATTGATCGAGAAGTCTAGATTGGATCTTGCTGGCAC
EXT2	M-EXT2-E13U	GGGTTCCCTAAGGGTTGGACAGCCATAGATGGGCTTTCACT
	M-EXT2-E13D	*AGACCAAACACACATGGTGGATCTAGATTGGATCTTGCTGGCAC
AMT	M-AMT-E1U	GGGTTCCCTAAGGGTTGGAGATGCAGAGGGCTGTAAGTGTGGTG
	M-AMT-E1D	*GCCCGTCTGCGCTTTCGCCTGTCTAGATTGGATCTTGCTGGCAC
	M-AMT-E4U	GGGTTCCCTAAGGGTTGGAAGGGCCACCTGTATGTGGTGTCCAAC
	M-AMT-E4D	*GCTGGCTGCTGCGGAGAAAGATTTTCTAGATTGGATCTTGCTGGCAC
	M-AMT-E9U-2	GGGTTCCCTAAGGGTTGGATGATGCGTGGCTTATGCTTGCTTGACAG
	M-AMT-E9D-2	*GTACTGTGACTAGTGGCTGCCCCTTCTAGATTGGATCTTGCTGGCAC

Single-underlined and double-underlined sequences are binding sites for forward and reverse polymerase chain reaction (PCR) primers, respectively.
*5′ phosphorylation.

A389V mutations in the *GLDC* gene was conducted. The study was approved by the Ethics Committee of Tohoku University School of Medicine, Sendai, Japan, and all patients or their legal representatives gave informed consent for DNA analysis.

Synthetic MLPA probes

In all, 29 pairs of MLPA probes were designed for analysis (table 1). As there is a processed pseudogene (*GLDCP*) which is 98% homologous with *GLDC* exons,[22] probes for the *GLDC* gene

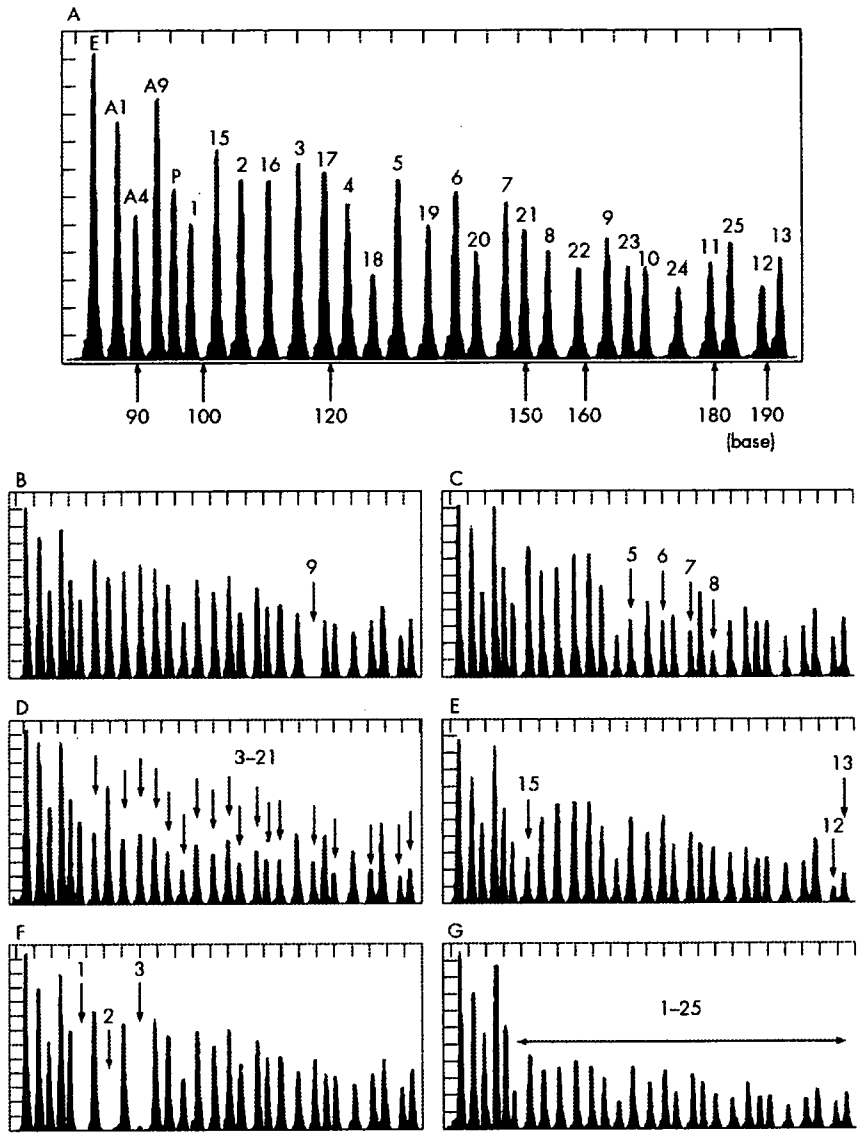

Figure 1 Multiplex ligation-dependent probe amplification (MLPA) analysis of a control subject and patients with non-ketotic hyperglycinaemia (NKH) with neonatal onset. A representative MLPA chromatogram of a control participant (A). The five control peaks include *EXT2* exon 13 (E), *AMT* exons 1, 4 and 9 (A1, A4, A9), and *GLDCP* (P). The number on each peak indicates the exon number of the *GLDC* gene. MLPA probe for *GLDC* exon 14 was not used in this assay. MLPA analysis of patients with NKH: homozygotic deletion of exon 9 (B), heterozygotic deletion of exons 5–8 (C), heterozygotic deletion of exons 3–21 (D), heterozygotic deletion of exons 12–15 (E), homozygotic deletion of exons 1–3 (F) and heterozygotic deletion of all 25 *GLDC* exons (G).

were placed at the 5′ or 3′ junction of each exon. No probe for exon 14 was used, as it lies only 175 bp from exon 13. Probes for *AMT* exons 1, 4 and 9, *EXT2* exon 13, and *GLDCP* were used as gene dose controls for estimation of *GLDC* copy number. The length of the synthetic MLPA probes ranged from 41 to 112 bp in size. Table 2 shows their nucleotide sequences. The probe for *EXT2* exon 13 was synthesised as reported previously.[24] We first tested the 3′ end of each exon as the target site. However, this did not work for *GLDC* exon 5, 18, 24 and *AMT* exon 9, so probes were designed at these 5′ regions of the exons. All downstream MLPA probes were 5′ phosphorylated for ligation with the upstream probes. The MLPA probe mixture was prepared by mixing 2 nmol/l of each MLPA probe, and used as described below.

MLPA procedures

An MLPA P0 FAM detection kit (MRC Holland, Amsterdam, The Netherlands) was used in this study. This kit contains all the necessary reagents except the MLPA probe mixture. MLPA was performed essentially according to the manufacturer's instructions (www.mrc-holland.com). Briefly, 50–250 ng of genomic DNA was used as the starting material, and after hybridisation, ligation and amplification, the PCR products were size-separated by an ABI 310 Genetic Analyzer (Applied Biosystems, Foster City, California, USA). For normalisation, relative peak areas were calculated by dividing each measured peak area by the sum of the five control peak areas (table 1). Mean and SD were obtained by testing 18 control DNA samples.

Table 3 *GLDC* deletions identified in patients with NKH

Deletion	Missing exons	Number of alleles	Family	Ethnicity	Other allele	Comment
First cohort (*AMT*-mutation negative, 45 families)						
1	Exons 1–2	2	P14	Caucasian	c.2714T→G (p.V905G)	
			P36	Caucasian	Deletion (exons 1–17)	
2	Exons 1–3	3	P5	Oriental	Deletion (exons 1–3)	Homozygote, consanguinity (−)
			P70	Oriental	Unidentified	
3	Exons 1–17	2	P36	Caucasian	Deletion (exons 1–2)	
			P40	Caucasian	Unidentified	
4	Exons 1–25	1	P32	Caucasian	c.1786C→T (p.R596X)	
5	Exons 3–4	1	P69	Oriental	c.2311G>A (p.G771R)	
6	Exons 3–8	1	P120	Oriental	c.2574T→G (p.Y858X)	
7	Exons 3–9	1	P47	Oriental	c.2519T→A (p.M840K)	
8	Exons 3–22	1	P48	Caucasian	c.2665+1G→C	
9	Exons 12–15	4	P7	Oriental	c.2266_2268del TTC	
			P8	Oriental	c.2080G→C (p.A694P)	
			P22	Oriental	Unidentified	
			P74	Oriental	c.2311G→A (p.G771R)	
Second cohort (not prescreened for *AMT* mutation, 20 families)						
1	Exon 1	1	B3	Caucasian	Unidentified	
2	Exons 1–2	2	B8	Caucasian	c.1545G→C (p.R515S)	
			B13	Caucasian	c.1545G→C (p.R515S)	
3	Exons 1–16	2	B10	Pakistani	Deletion (exons 1–16)	Homozygote, consanguinity (+)
4	Exons 3–21	1	B6	Caucasian	Unidentified	
5	Exon 9	2	B7	Caucasian	Deletion (exon 9)	Homozygote, consanguinity (+)
6	Exons 5–8	1	B18	Caucasian	c.1545G→C (p.R515S)	

Long-range PCR

To clarify the boundary sequences of the deleted fragments, we used nested and long-range PCR with the LA PCR kit (TaKaRa Co Ltd, Tokyo, Japan) for PCR across the breakpoints. PCR fragments containing the boundary sequences of the deletions were size-separated on 1% agarose gel and bands with the expected sizes were cut out for purification by the QIAquick Gel Extraction kit (Qiagen, Hilden, Germany). Purified PCR fragments were subjected to the dye-terminator-sequencing analysis with the BigDye Terminator Sequencing Kit (Applied Biosystems).

RESULTS

MPLA analysis in control DNA

Eighteen control DNA samples were tested to estimate the deviation of each peak area. Figure 1A shows a representative chromatogram with all 29 peaks. Intervals between the peaks correspond to a difference of three or four bases in size of DNA fragments. Each peak area was measured and the mean (SD) was calculated (table 1). The sum of the five control peak areas (*EXT2* exon 13, *AMT* exons 1, 4 and 9, and *GLDCP*) was used to normalise the relative peak area of each *GLDC* exon. As a result, the mean (SD) ranged from 2% to 6%. We therefore set a screening threshold for deletion as <80%, <−3 SD from the mean value.

MPLA analysis in patients with NKH

Two independent cohorts of patients with neonatal-onset NKH were screened by our MLPA system. Nine different types of *GLDC* deletions were detected in the first *AMT*-mutation negative cohort of patients, whereas six different types of deletions were found in the second cohort of patients, in which no prescreening of *AMT* mutation had been performed (table 3). Figure 1 shows six representative results of *GLDC* deletions: homozygotic deletion of exon 9 (fig 1B), heterozygotic deletion of exons 5–8 (fig 1C), heterozygotic deletion of exons 3–21 (fig 1D), heterozygotic deletion of exons 12–15 (fig 1E), homozygotic deletion of exons 1–3 (fig 1F) and heterozygotic deletion involving all 25 *GLDC* exons (fig 1G). In the first cohort, a total of 16 deletion alleles were identified in 90 mutant alleles (18%). In the second cohort, 9 of 40 (22.5%) alleles were positive for deletion screening. No deletions of *AMT* exons 1, 4 and 9 were detected in this study. MLPA analysis of family P41 suggested that the patient was homozygotic for a deletion of exon 7 (data not shown). Subsequent sequencing analysis of the probe binding sites disclosed a one-bp deletion, c.1054delA, in the M-GLDC-E7U binding site. Similarly, in the MLPA analysis of family B5, both parents appeared to be heterozygotic for a deletion of exon 5 (data not shown). Sequencing of the probe binding sites showed that this was due to a single base substitution in the M-GLDC-E5U-2 binding site on one allele. Unfortunately, no DNA was available from the index case, but the patient from family B5 was presumed to be homozygotic for this c.636-1G→C mutation, which was deduced to abolish the conserved consensus AG at the splicing acceptor sites.

Identification of boundary sequences of the deletions

To confirm the deletions identified by the MPLA study and elucidate the mechanisms of the deletions, we examined the boundary sequences of four interstitial deletions within *GLDC*. We examined the patient homozygotic for a deletion of exon 9 (family B7 in the second cohort), the patient with heterozygotic deletion of exons 5–8 (family B18 in the second cohort), the patient with heterozygotic deletion of exons 3–21 (family B6 in the second cohort) and the patients with heterozygotic deletions of exons 12–15 (families P74 and P8 in the first cohort; fig 2). Nested long-range PCR was employed in this analysis, which was followed by direct sequencing analysis. In the patient of family B7, a 7906-bp deletion was identified, extending from the 3′ end of intron 8 (~6 kb) to the 5′ end of intron 9 (~2 kb) as shown in fig 2A. In the patient in family B18, we found a 10 422-bp deletion beginning at the 3′ end of intron 4 (~3 kb) and including exons 5–8, up to the 5′ end of intron 8 with ~3 kb (fig 2B). The patient in family B6 had the longest deletion, 99 395 bp, among the four patients. Both 5′

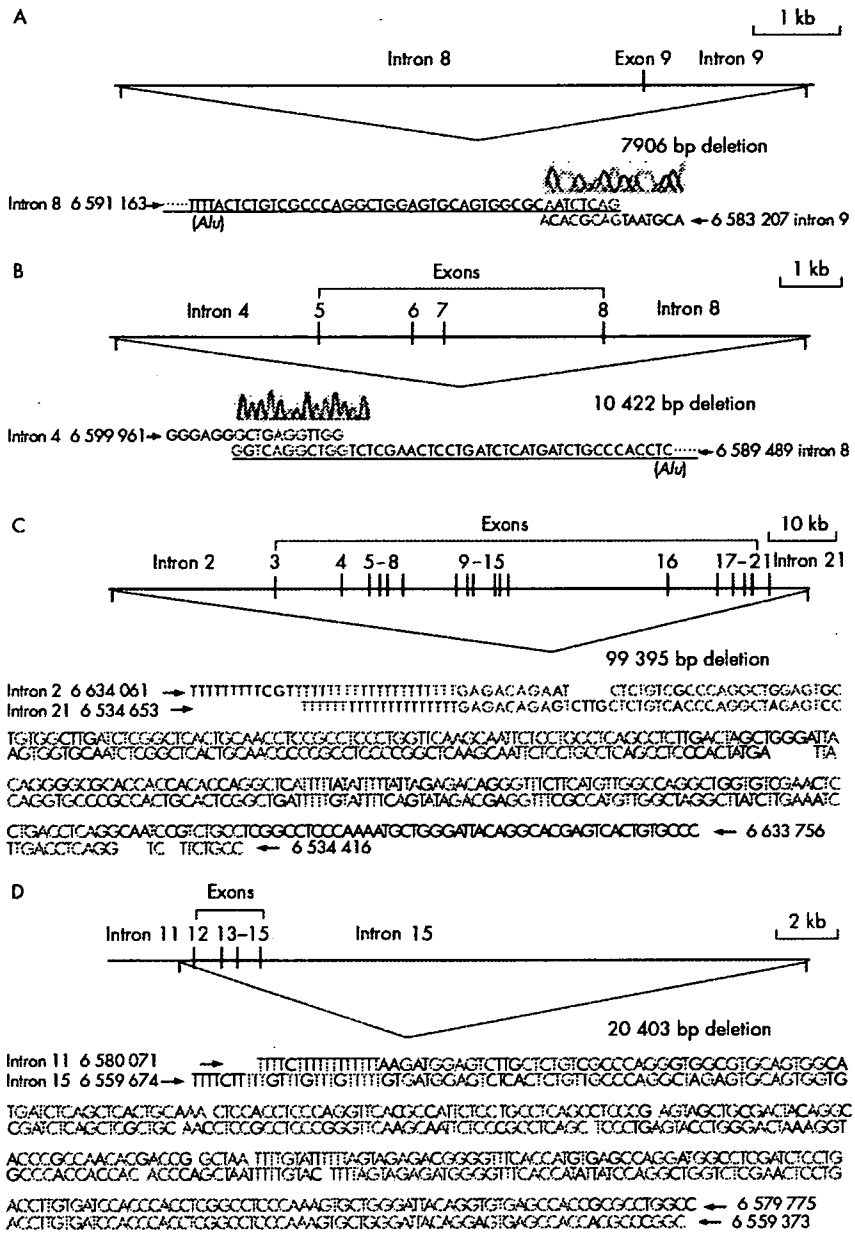

Figure 2 Boundary sequences of the deleted fragments. The boundary sequences of four different types of *GLDC* deletions were identified: the deletion of exon 9 in family B7 (A), the deletion of exons 5–8 in family B18 (B), the deletion of exons 3–21 in family B6 (C) and the deletion of exons 12–15 in family P74 (D). The boundary sequence found in family P74 was the same as that in family P8. Nucleotide sequences in red indicate the identical bases in the 5′ and 3′ flanks of the deletions.

and 3′ fragments shared near identical sequences as shown in fig 2C. In a Japanese patient (P74) with heterozygotic deletion of exons 12–15, a 20 403-bp deletion was identified (fig 2D). The deleted fragment consisted of a short 3′ end of intron 11 (~0.6 kb), exons 12–15 and the 5′ end of intron 15 (~18 kb). The identical breakpoint was also found in the patient from family P8 (data not shown). Thus far, the deleted fragments flanked with *Alu* motifs in B6, P74, and P8 patients, but not in patients from families B7 or B18. Four Caucasian patients (from P14, P36, B13 and B8) had a deletion of exons 1 and 2. However, as the two patients, B13 and B8, from the UK had different haplotypes (data not shown), this deletion has occurred more than once. This observation agrees with our previous finding that the deletions of the *GLDC* exon 1 had multiple origins.[21]

Distribution of deletions in the *GLDC* gene

Figure 3 shows the distribution of the missing exons by *GLDC* deletions. The lengths of the *GLDC* deletions were heterogeneous, ranging from a single exon to all 25. Of the 50 breakpoints of the deletions, 26 (52%) were found 5′ upstream of the *GLDC* gene or in introns 1–3, suggesting that deletions

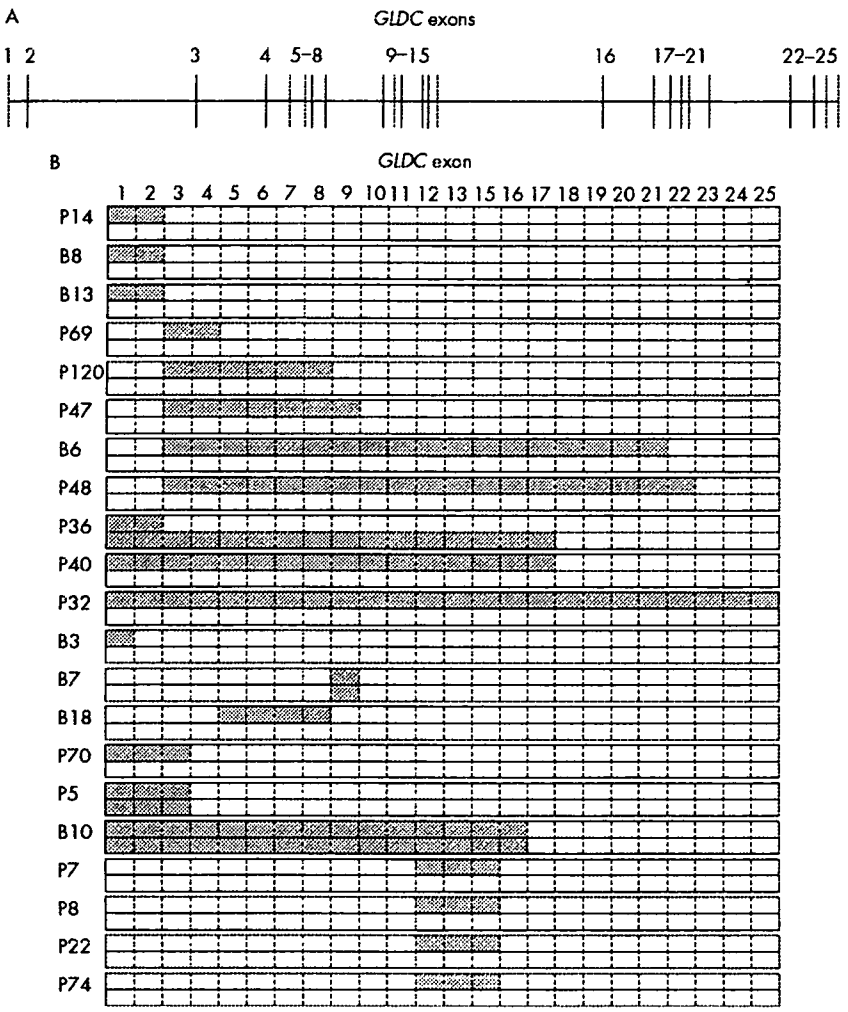

Figure 3 Distribution of missing exons by the *GLDC* deletions. The exon–intron organisation of the *GLDC* gene is illustrated (A). Patients with non-ketotic hyperglycinaemia with *GLDC* deletions were classified by their missing exons (B). Hatched boxes indicate *GLDC* exons involved in the deletions. Note the clustering of the deletion breakpoints in the 5′ end of *GLDC*.

tend to occur in the 5′ part of the *GLDC* gene, a region relatively rich in *Alu* repeats.

DISCUSSION

We established a detection system for *GLDC* deletions by using the MLPA method, and showed that deletions within this gene are a common cause of NKH. Fourteen different types of *GLDC* deletions were identified in screening 65 patients with neonatal-onset NKH. *GLDC* deletions were identified in 21 of 65 patients with NKH (32.3%), and in 25 of 130 NKH alleles (19.2%) by MLPA analysis. The MLPA method provides a good first-line screen in a condition where there are no common mutations and full sequencing of 25 exons of the *GLDC* gene is a lengthy process. The deletion detection rates by MLPA analysis were 18% and 22.5% in the first and second cohorts, respectively. In our previous study, the exon-sequencing analysis has shown *GLDC* mutations in 41 of 90 alleles (45%).[21] Thus, this MLPA test improved the sensitivity of mutation detection from 45% to 63%. Mutations for NKH are highly heterogeneous: the prevalent mutations previously reported are Finnish S564I mutation (70%)[14] and Caucasian R515S mutation (5%),[15] hampering the genetic testing in diagnosis of NKH. In contrast, *GLDC* deletions seem to be prevalent in different ethnic groups. In a previous study, we analysed the relative allele number of the *GLDC* exon 1 by using *GLDCP* as a copy number control.[22] As MLPA analysis covers the whole gene in one simple assay, it is highly recommended for the first screening in the genetic testing of NKH.

Point mutations in MLPA-probe binding sites may cause false positives in MLPA analysis, notably where a single exon is deleted. A mismatching in the binding site of the MLPA probes is known to reduce the ligation efficiency. In our study, we encountered four single-exon deletions in the analysis of families P41, B3, B5 and B7. Subsequent sequencing analysis of the probe binding sites showed that the patient in family P41 had a 1-bp deletion and that the patient from B5 carried a 1-base substitution at the splicing accepter site of intron 4. Both mutations are predicted to be disease causing. No base change was found in the patient from B3. In the patient from B7, exon 9 of the patient failed to be amplified by PCR and a single-exon deletion was confirmed by subsequent sequencing across the breakpoint (fig 2A). As the MLPA probes for *GLDC* were

Key points

- A screening system for genomic deletions within *GLDC* has been developed by the multiplex-ligation-dependent probe amplification (MLPA) method
- *GLDC* deletions were identified in approximately 20% of non-ketotic hyperglycinaemia (NKH) mutant alleles.
- The MLPA analysis is useful for first-line screening in the genetic testing of NKH.

designed to bind an exon–intron boundary to avoid detection of the pseudogene of *GLDC*, *GLDCP*, the MLPA method can also detect some mutations that cause aberrant splicing. Sequencing the probe-binding regions of the *GLDC* gene where MLPA analysis suggests a single-exon deletion is therefore necessary before making a diagnosis of *GLDC* deletion.

In a previous study, we diagnosed the patient of family P32 as a homozygote of a nonsense mutation, c.1786C→T (p.R596X), although there was no history of consanguinity.[21] A familial study was not possible because no parental DNA was available. The present study showed that he was heterozygotic for a deletion containing all 25 *GLDC* exons (table 3, fig 1G), indicating that he was a compound heterozygote of the nonsense mutation c.1786C→T and the deletion of exons 1–25. As this deletion was the biggest one so far identified, we looked to see whether it involved any adjacent genes. We performed a microarray analysis to determine the genotypes of many single-nucleotide polymorphisms (SNPs) by using the GeneChip Human Mapping 100 k Set (Affymetrix, Santa Clara, California, USA). *GLDC* is located between base positions 6635650 and 6522467 bp in chromosome 9 (GenBank, NT_008413). The JMJD2C gene (6748083–7165647 bp) is located 5′ upstream of *GLDC* whereas the UHRF2 gene (6403151–6497051 bp) lies 3′ downstream of *GLDC*. The SNP at the base position 6606648 bp, which is located within the *GLDC* gene, was indeed homozygotic in this patient (data not shown). In contrast, two SNPs at the base positions of 6513056 and 6759229 bp were heterozygotic, suggesting that the deletion is <246 kb, and thus that the two adjacent genes are unlikely to be involved in the deletion.

We determined flanking sequences of interstitial deletions in five patients, and *Alu*-mediated recombination was identified in three of five patients. The *Alu* elements, approximately 300 bp in length, compose about 10% of the whole human genome.[25] There are several inherited disorders in which *Alu*-mediated recombination/deletion is a common cause: hereditary angioedema, *C1-INH*;[26] α-thalassemia, α-globin gene;[27] and Ehlers–Danlos syndrome, *PLOD*.[28] Recently, *Alu*-mediated genomic recombination has also been reported in non-inherited human cancer, hepatoma.[29] A total of 120 copies of *Alu* repeats are present in the *GLDC* gene, which has a length of 113 kb, resulting in one *Alu* of 1.1 kb on average. This is much higher than the average density of one *Alu* every 3–4 kb over the whole human genome.[10] The *GLDC* deletions tend to be located in the 5′ end of the *GLDC* gene, which may be explained by the fact that the region contains a high number of *Alu* repeats.

The diagnosis of NKH is difficult to establish on clinical and biochemical grounds alone, and typically requires a liver biopsy for enzyme analysis or DNA studies to confirm a diagnosis. However, the complex nature of the genetics of NKH (three genes and no common mutations) makes DNA analysis a lengthy and difficult process. Our finding that deletions within the *GLDC* gene are one of the most common causes of NKH and the development of a simple assay for such mutations will make genetic analysis for this disorder much more straightforward. Such analysis will reduce the need for a liver biopsy in a sick child, make diagnosis easier, and improve the ease and reliability of antenatal diagnosis.

ACKNOWLEDGEMENTS

We thank all the families who participated in this study.

Authors' affiliations
Junko Kanno, Fumiaki Kamada, Ayumi Narisawa, Yoko Aoki, Yoichi Matsubara, Shigeo Kure, Department of Medical Genetics, Tohoku University School of Medicine, Sendai, Japan
Tim Hutchin, Department of Clinical Chemistry, Birmingham Children's Hospital, Birmingham, UK

Funding: This work was supported by a grant from the Ministry of Education, Culture, Sports, Science, and Technology and the Ministry of Health, Labor and Welfare in Japan. Funding was also provided by the Robert Gaddie Memorial Fund and from the Tohoku University 21st COE Program "Comprehensive Research and Education Center for Planning of Drug Development and Clinical Evaluation", Sendai, Japan.

Competing interests: None declared.

Electronic databases: NKH (GCE)-OMIM, 605899. *GLDC*-OMIM: 238300, GenBank: NT_008413.

Correspondence to: Dr S Kure, Department of Medical Genetics, Tohoku University School of Medicine, 1-1 Seiryomachi, Aobaku, Sendai 980-8574, Japan; skure@mail.tains.tohoku.ac.jp

Received 19 April 2006
Revised 13 June 2006
Accepted 17 June 2006

REFERENCES

1 **Hamosh A**, Johnston MV. Nonketotic hyperglycinemia. In: Scriver CR, Beaudet AL, Sly WS, *et al*, eds. *The metabolic and molecular bases of inherited disease*. 8th edn, Vol 2. New York: McGraw-Hill, 2001:2065–78.
2 **Kure S**, Tada K, Narisawa K. Nonketotic hyperglycinemia: biochemical, molecular, and neurological aspects. *J Hum Genet* 1997;**42**:13–22.
3 **Tada K**, Kure S. Nonketotic hyperglycinemia: pathophysiological studies. *Proc Japan Acad* 2005;**81**(Ser B):411–17.
4 **Hoover-Fong JE**, Shah S, Van Hove JL, Applegarth D, Toone J, Hamosh A. Natural history of nonketotic hyperglycinemia in 65 patients. *Neurology* 2004;**63**:1847–53.
5 **Dinopoulos A**, Kure S, Chuck G, Sato K, Gilbert DL, Matsubara Y, Degrauw T. Glycine decarboxylase mutations: a distinctive phenotype of nonketotic hyperglycinemia in adults. *Neurology* 2005;**64**:1255–7.
6 **Flusser H**, Korman SH, Sato K, Matsubara Y, Galil A, Kure S. Mild glycine encephalopathy (NKH) in a large kindred due to a silent exonic GLDC splice mutation. *Neurology* 2005;**64**:1426–30.
7 **Korman SH**, Wexler ID, Gutman A, Rolland MO, Kanno J, Kure S. Treatment from birth of nonketotic hyperglycinemia due to a novel GLDC mutation. *Ann Neurol* 2006;**59**:411–15.
8 **Tada K**, Narisawa K, Yoshida T, Yokoyama K, Nakagawa H, Tanno K, Mochizuki K, Arakawa T, Yoshida T, Kikuchi G. Hyperglycinemia: a defect in glycine cleavage reaction. *Tohoku J Exp Med* 1969;**98**:289–96.
9 **Kikuchi G**. The glycine cleavage system: composition, reaction mechanism, and physiological significance. *Mol Cell Biochem* 1973;**1**:169–87.
10 **Isobe M**, Koyata H, Sakakibara T, Momoi-Isobe K, Hiraga K. Assignment of the true and processed genes for human glycine decarboxylase to 9p23–24 and 4q12. *Biochem Biophys Res Commun* 1994;**203**:1483–7.
11 **Nanao K**, Takada G, Takahashi E, Seki N, Komatsu Y, Okamura-Ikeda K, Motokawa Y, Hayasaka K. Structure and chromosomal localization of the aminomethyltransferase gene (AMT). *Genomics* 1994;**19**:27–30 (published erratum appears in *Genomics* 1994;**20**:519).
12 **Kure S**, Kojima K, Kudo T, Kanno K, Aoki Y, Suzuki Y, Shinka T, Sakata Y, Narisawa K, Matsubara Y. Chromosomal localization, structure, single-nucleotide polymorphisms, and expression of the human H-protein gene of the glycine cleavage system (GCSH), a candidate gene for nonketotic hyperglycinemia. *J Hum Genet* 2001;**46**:378–84.
13 **Tada K**. Nonketotic hyperglycinemia: clinical and metabolic aspects. *Enzyme* 1987;**38**:27–35.
14 **Kure S**, Takayanagi M, Narisawa K, Tada K, Leisti J. Identification of a common mutation in Finnish patients with nonketotic hyperglycinemia. *J Clin Invest* 1992;**90**:160–4.
15 **Toone JR**, Applegarth DA, Coulter-Mackie MB, James ER. Biochemical and molecular investigations of patients with nonketotic hyperglycinemia. *Mol Genet Metab* 2000;**70**:116–21.